MIXv2: a long-term mosaic emission inventory for Asia (2010-2017)

Meng Li[1,2], Junichi Kurokawa[3], Qiang Zhang[4], Jung-Hun Woo[5,6], Tazuko Morikawa[7], Satoru Chatani[8], Zifeng Lu[9], Yu Song[10], Guannan Geng[11], Hanwen Hu[11], Jinseok Kim[6], Owen R. Cooper[1,2], Brian C. McDonald[2]

[1] Cooperative Institute for Research in Environmental Sciences, University of Colorado, Boulder, CO, USA

[2] NOAA Chemical Sciences Laboratory, Boulder, CO, USA

[3] Asia Center for Air Pollution Research, 1182 Sowa, Nishi-ku, Niigata, Niigata, 950-2144, Japan

[4] Ministry of Education Key Laboratory for Earth System Modeling, Department of Earth System Science, Tsinghua University, Beijing, China

[5] Department of Civil and Environmental Engineering, Konuk University, Seoul, Republic of Korea

[6] Department of Technology Fusion Engineering, Konkuk University, Seoul, Republic of Korea

[7] Japan Automobile Research Institute, 2530 Karima, Tsukuba, Ibaraki, 305-0822, Japan

[8] National Institute for Environmental Studies, 16-2 Onogawa, Tsukuba, Ibaraki, 305-8506, Japan

[9] Energy Systems and Infrastructure Analysis Division, Argonne National Laboratory, Lemont, IL, USA

[10] State Key Joint Laboratory of Environmental Simulation and Pollution Control, Department of Environmental Science, Peking University, Beijing, People's Republic of China

[11] State Key Joint Laboratory of Environmental Simulation and Pollution Control, School of Environment, Tsinghua University, Beijing, China

Correspondence to: Meng Li (Meng.Li-1@colorado.edu)

Abstract

The MIXv2 Asian emission inventory is developed under the framework of the Model Inter-
Comparison Study for Asia (MICS-Asia) Phase IV, and produced from a mosaic of up-to-date
regional emission inventories. We estimated the emissions for anthropogenic and biomass
burning sources covering 23 countries and regions in East, Southeast and South Asia, and
aggregated emissions to a uniform spatial and temporal resolution for seven sectors: power,
industry, residential, transportation, agriculture, open biomass burning and shipping. Compared
to MIXv1, we extended the dataset to 2010 – 2017, included emissions of open biomass burning
and shipping, and provided model-ready emissions of SAPRC99, SAPRC07, and CB05. A series
of unit-based point source information was incorporated covering power plants in China and
India. A consistent speciation framework for Non-Methane Volatile Organic Compounds
(NMVOCs) was applied to develop emissions by three chemical mechanisms. The total Asian
emissions for anthropogenic | open biomass sectors in 2017 are estimated as follows: 41.6 | 1.1
Tg NO_x, 33.2 | 0.1 Tg SO_2, 258.2 | 20.6 Tg CO, 61.8 | 8.2 Tg NMVOC, 28.3 | 0.3 Tg NH_3, 24.0 |
2.6 Tg PM_{10}, 16.7 | 2.0 Tg $PM_{2.5}$, 2.7 | 0.1 Tg BC, 5.3 | 0.9 Tg OC, and 18.0 | 0.4 Pg CO_2. The
contributions of India and Southeast Asia have been emerging in Asia during 2010-2017,
especially for SO_2, NH_3 and particulate matters. Gridded emissions at a spatial resolution of 0.1
degree with monthly variations are now publicly available. This updated long-term emission
mosaic inventory is ready to facilitate air quality and climate model simulations, as well as
policy-making and associated analyses.

1. Introduction

Air pollutants emitted from both anthropogenic and natural activities have caused severe impacts
on human health, ecosystems, and climate over Asia (Adam et al., 2021; Geng et al., 2021;
Takahashi et al., 2020; Wong et al., 2008; Xie et al., 2018). Over the last two decades, the
emerging ozone pollution and haze events across Asia have got extensive attention from the
government (Anwar et al., 2021; Feng et al., 2022; Zheng et al., 2018). Tremendous efforts have
been made since 2010 continuously to improve air quality and protect human health. The effects
of these policies on emission abatement need to be updated in inventories, to address the regional
and global issues of air quality and climate change. Therefore, a long-term emission inventory
plays key roles in historical policy assessment, and future air quality and climate mitigation.

Consistent greenhouse gas emissions are crucial for climate-air quality nexus research and
policymaking (Fiore et al., 2015). Carbon dioxide (CO_2) is co-emitted with many air pollutants
which are contributors of ozone and particulate matter, further changing climate through forcings
of Earth's radiation budget (Fiore et al., 2015). Previous studies have emphasized the importance
of air pollution mitigation and climate change (Jacob and Winner, 2009; Saari et al., 2015), as
recently summarized by the Synthesis Report of the IPCC Sixth Assessment Report (IPCC:
Intergovernmental Panel on Climate Change, report available at
https://www.ipcc.ch/report/sixth-assessment-report-cycle/). Given the common sources of CO_2
and air pollutants, it's important to quantify their emissions distribution in a self-consistent way

2

71 to assess the co-benefits and pathways to cleaner air and carbon neutrality (Klausbruckner et al.,
72 2016; Phillips, 2022; von Schneidemesser and Monks, 2013).

73 Emissions over Asia since 2010 are quantified in recent studies. Kurokawa et al. (2020)
74 developed an anthropogenic emission inventory over Asia for 1950-2015, REAS (the Regional
75 Emission inventory in ASia), covering power plants, industry, residential, transportation and
76 agricultural sources. Emissions of both air pollutants and CO_2 are estimated in REAS. Based on
77 the Community Emissions Data System (CEDS), McDuffie et al. (2020) developed a global
78 anthropogenic emission inventory covering major air pollutants over 1970-2017. Global
79 emissions for air pollutants are estimated under the HTAPv3 (Task Force on Hemispheric
80 Transport of Air Pollution) project for 2000-2018 for air pollutants by integrating official
81 inventories over specific areas including Asia (Crippa et al., 2023). These regional / global
82 emissions are estimated with limited updates of country-specific or even localized information.
83 Following a mosaic approach, the first version of MIX Asian inventory (MIXv1) was developed
84 to support the Model Inter-Comparison Study for Asia (MICS-Asia) Phase III projects, by
85 incorporating five regional emission inventories for all major anthropogenic sources over Asia,
86 providing a gridded emission dataset at a spatial resolution of 0.25 degree for 2008 and 2010.
87 The mosaic approach has been proved to increase the emission accuracy and model performance
88 significantly by including more local information (Li et al., 2017c). A profile-based speciation
89 scheme for Non-Methane Volatile Organic Compounds (NMVOCs) was applied to develop
90 model-ready emissions by chemical mechanisms, which reduced the uncertainties arising from
91 inaccurate mapping between inventory and model species (Li et al., 2014; Li et al., 2019b).
92 Specifically, MIXv1 advances our understanding of emissions and spatial distributions from
93 power plants through a mosaic of unit-based information, and agricultural activities based on a
94 process-based model which parameterized the spatial and temporal variations of emission factors
95 for NH_3.

96 However, it's difficult to develop consistent emissions over Asia for a long period using the
97 mosaic approach because of the lack of available regional inventory data. Within the MICS-Asia
98 community, developers of regional inventories have been endeavoring to extend their emission
99 inventories to the present day since Phase IV. Through intensive collaboration and community
100 efforts, we now have a complete list of available regional emission inventories covering major
101 parts of Asia, and are able to combine them to produce a new version of MIX for 2010-2017.
102 MICS-Asia is currently in its fourth phase, MICS-Asia IV, which aims to advance our
103 understanding of the discrepancies and relative uncertainties present in the simulations of air
104 quality and climate models (Chen et al., 2019; Gao et al., 2018; Itahashi et al., 2020; Li et al.,
105 2017c). A critical component of the project is ensuring that emission inventories remain
106 consistent across various atmospheric and climate models. In support of MICS-Asia IV research
107 activities and related policy-making endeavors, we developed MIXv2, the second version of our
108 mosaic Asian inventory. MIXv2 combines the best available state-of-the-art regional emission
109 inventories from across Asia using a mosaic approach. This inventory is expected to enhance our
110 capabilities to assess emission changes and their driving forces, and their impact on air quality
111 and climate change, thus providing valuable insights for decision-makers and stakeholders. CO_2

112 emissions are estimated based on the same emission inventory framework as the short-lived air
113 pollutants, and further integrated into MIXv2 following the mosaic methodology.

114 MIXv1 has been widely applied to support scientific research activities from regional to local
115 scales (Geng et al., 2021; Hammer et al., 2020; Li et al., 2019a; Li et al., 2017c). Compared to
116 MIXv1, MIXv2 has the following updates to better feed the needs of atmospheric modelling
117 activities:

118 - advances the horizontal resolution of the gridded maps from 0.25 to 0.1 degree

119 - incorporates up-to-date regional inventories from 2010-2017

120 - provides emissions of open biomass burning and shipping, in addition to anthropogenic sources

121 - develops model-ready emissions of SAPRC99, SAPRC07 and CB05

122 Methods and input data are described in Sect. 2. Emissions evolution and their driving forces,
123 seasonality, spatial distribution, NMVOC speciation and inventory limitations are analyzed and
124 discussed in Sect. 3. Sect. 4 compares the MIX data with other bottom-up and top-down
125 emission estimates. Concluding remarks are provided in Sect. 5.

126

127 2. Methods and Inputs

128 2.1 Overview of MIXv2

129 The key features of MIXv2 are summarized in Table 1. Anthropogenic sources, including power,
130 industry, residential, transportation and agriculture, along with open biomass burning and
131 shipping are included. Dust and aviation are not included in the current version of MIX. Monthly
132 emissions between 2010 – 2017 are allocated to grids at 0.1×0.1 degree. Open biomass burning
133 emissions are also available with daily resolution upon request. Emissions of ten species,
134 including CO_2 and air pollutants of NO_x, SO_2, CO, NMVOC, NH_3, PM_{10}, $PM_{2.5}$, BC and OC are
135 estimated. MIX can support most atmospheric models compatible with gas-phase chemical
136 mechanisms of SAPRC99, SAPRC07, CB05, and those can be mapped based on these three
137 chemical mechanisms (e.g., GEOS-Chem, MOZART) (Li et al., 2014). As shown in Figure 1,
138 MIXv2 stretches from Afghanistan in the west to Japan in the east, from Indonesia in the south to
139 Mongolia in the north. The domain is consistent with the REASv3 gridded emissions product.

140 Table 2 summarizes the subsectors for each sector in the development of MIX, along with the
141 corresponding source codes used by IPCC.

142

143 2.2 Mosaic Methodology

144 We follow a mosaic methodology similar to the development of MIXv1 (Li et al., 2017c), as shown
145 in Figure 1. In brief, nine regional and two global emission inventories were collected and
146 integrated into a uniform format, including: REAS version 3 for Asia (referred to as REASv3)

147 (Kurokawa and Ohara, 2020); the Multi-resolution Emission Inventory for China version 2.0
148 (MEICv2, http://www.meicmodel.org) (Li et al., 2017b; Zheng et al., 2021; Zheng et al., 2018); a
149 process-based NH_3 emission inventory developed by Peking University (referred to as PKU-NH_3)
150 (Kang et al., 2016); an official Japan emission inventory (referred to as JPN) (Chatani et al., 2018;
151 Shibata and Morikawa, 2021); an Indian emission inventory for power plants from Argonne
152 National Laboratory (referred to as ANL-India) (Lu and Streets, 2012; Lu et al., 2011); an open
153 biomass burning emission inventory from Peking University (PKU-Biomass) (Yin et al., 2019);
154 the official emissions from Clean Air Policy Support System (CAPSS) for the Republic of Korea
155 (Lee et al., 2011) ; the fourth version of Global Fire Emissions Database with small fires
156 (GFEDv4s) (van der Werf et al., 2017); and the Emissions Database for Global Atmospheric
157 Research (EDGAR) version 6 for the shipping emissions (Janssens-Maenhout et al., 2019). Figure
158 1 shows the distribution of the components of emission inventories which are mosaicked into the
159 MIXv2.
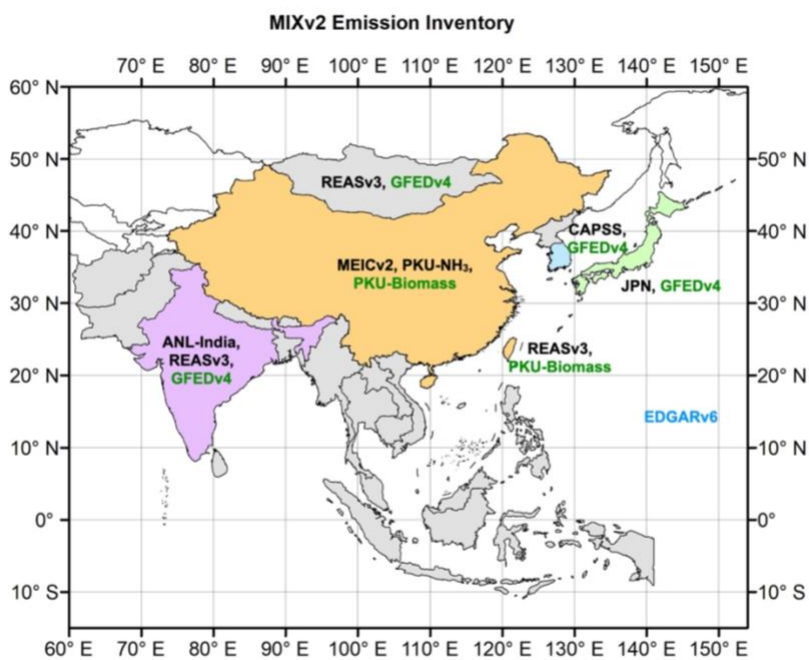
160
161 **Figure 1. Components of regional emission inventories in the MIXv2 mosaic. Colors of text**
162 **represent the type of sources: black is anthropogenic, dark green represents open biomass**
163 **burning, and blue is the inland and international shipping.**

164

165 We follow a similar hierarchy in MIXv2 as the previous version in the mosaic process. We use
166 REASv3 as the default inventory for anthropogenic sources, and then further replace it with
167 official emission inventories at a finer scale. MEIC, PKU-NH_3 and ANL-India are demonstrated
168 as the best available inventories through inter-comparisons to represent local source distribution
169 with advanced methodology and reliable data sources (Li et al., 2017c). Thus, MEIC overrides
170 REAS for anthropogenic emissions over mainland China. PKU-NH_3, which was developed with

5

171 a process-based model was further applied to replace the NH_3 emissions in MEIC. In Japan, JPN
172 provides emissions for all air pollutants. The ratios of CO_2 to NO_x by sectors derived from REAS
173 are combined with JPN to develop CO_2 gridded emissions. In detail, we firstly calculated the
174 total CO_2 emissions of Japan by multiplying the CO_2 to NO_x ratios and JPN's NO_x emission
175 estimates by sectors, then we developed the spatial proxies based on the NO_x gridded emissions
176 of JPN. Lastly, the calculated CO_2 emissions were allocated to each grid month by month. We
177 use ANL-India for SO_2, NO_x and CO_2 for power plants in India directly, and complement
178 emissions of other species and sectors with REASv3. Regarding Hong Kong of China, we use
179 the updated REASv3 emissions.

180 The open biomass emissions of MIX are developed by combining GFEDv4s and PKU-Biomass
181 inventories. GFED emissions over Asia are processed to the objective domain. We re-gridded the
182 GFED emissions from 0.25 to 0.1 degree based on an area-weighted algorithm in a mass-
183 balanced way. Wildfires of various vegetation types (including savanna, forest, peatland) and in-
184 field agricultural waste burning are aggregated into the "open biomass burning" sector. PKU-
185 Biomass overrides the emissions of GFED over China (including Hong Kong and Taiwan) on a
186 both monthly and daily basis.

187 The consistency of data is ensured in three aspects: source aggregation, spatial distribution, and
188 NMVOC speciation. Firstly, a consistent source definition system was applied in source
189 aggregation from regional emission inventories to the final emission mosaic, as outlined in Table
190 2 and Table S1. Secondly, the consistency of emissions spatial distribution during emissions
191 mosaic between different inventories are ensured carefully. In India, we integrated the ANL-
192 India emissions for NO_x, SO_2, and CO_2 for pointed power plants, and emissions from REAS for
193 other species. To keep the consistency in spatial distribution, we developed spatial proxies based
194 on the CO_2 emissions from ANL-India, and re-located REAS emissions for other species.
195 Thirdly, a consistent NMVOC speciation framework was applied throughout all component
196 emission inventories for both anthropogenic and open biomass burning sources, which is
197 described in detail in Sect. 2.4.

Table 1. Key features of MIXv2 and the component emission inventories.

Items	MIXv2	REASv3.3	MEICv2.0	PKU-NH$_3$	ANL-India	JPN	CAPSS	PKU-Biomass	GFEDv4s	EDGARv6
Anthropogenic										
Power	X	X	X	X	X	X	X			
Industry	X	X	X	X		X	X			
Residential	X	X	X	X		X	X			
Transportation	X	X	X	X		X	X			
Agriculture	X	X	X	X		X	X			
Open biomass burning	X						X	X	X	
Shipping	X									X
Temporal coverage	2010-2017	1950-2017	1990-2017	1980-2017	2010-2017	2000-2017	2000-2018	1980-2017	2010-2017	1970-2018
Temporal resolution	Monthly	Monthly	Monthly	Monthly	Monthly	Monthly	Annual	Daily	Daily	Monthly
Spatial coverage	Asia	Asia	Mainland China	Mainland China	India	Japan	Korea, Republic of	China	Global	Global
Spatial resolution (degree in horizontal)	0.1	0.1, point	0.1, point	0.1	point	0.1	0.1	0.1	0.25	0.1
Species										
NO$_x$	X	X	X		X	X	X	X	X	X
SO$_2$	X	X	X		X	X	X	X	X	X
CO	X	X	X			X	X	X	X	X
NMVOC	X	X	X			X	X	X	X	X

NH₃	X	X	X	X	X	X	X	X
PM₁₀	X	X	X		X	X	X	X
PM₂.₅	X	X	X		X	X	X	X
BC	X	X	X		X	X	X	X
OC	X	X	X		X	X	X	X
CO₂	X	X	X	X		X	X	X
NMVOC speciation	SAPRC99, SPARC07, CB05	19 species	SAPRC99, SPARC07, CB05	N/A	SAPRC07, CB05	N/A	26 species	N/A
Data availability	https://csl.noaa.gov/groups/csl4/modeldata/data/Li2023/	https://www.nies.go.jp/REAS/index.html (for REASv3.2.1) (last access: 04/2022)	www.meicmodel.org (last access: 06/2022)	Lu et al. (2011) http://meicmodel.org.cn/?page_id=1772&lang=en (last access: 06/2022)	Chatani et al. (2018); Shibata and Morikawa (2021)	National Institute of Environmental Research Center http://meicmodel.org.cn/?page_id=1772&lang=en (last access: 06/2022)	https://www.globalfiredata.org/ (last access: 10/2022)	https://edgar.jrc.ec.europa.eu/ (last access: 10/2022)

200

201

202

203

204

205

206 **Table 2. Sector and subsectors included in MIXv2[a].**

Sector	Subsector	IPCC code[b]
Power	Power plants	1A1a
Industry	Industrial coal combustion	1A2, 1A1c
	Industrial other fuel combustion	1A2
	Chemical industry	1B2b, 2B
	Oil production, distribution, and refinery	1B2a
	Other industrial process	2A1, 2A2, 2A7, 2C, 2
	Industrial paint use	3A
	Solvent use other than paint	3B, 3C
Residential	Residential coal combustion	1A4b
	Residential biofuel combustion	1A4bx
	Residential other fuel combustion	1A4b
	Waste treatment	6A, 6C
	Domestic solvent use	3C
Transportation	On-road gasoline	1A3b
	On-road diesel	1A3b
	Off-road diesel	1A3c, 1A4c
Agriculture	Livestock	4B
	Fertilizer use	4D
Open biomass burning	Agriculture in-field burning	4F
	Fires	4E, 5A, 5C, 5D
Shipping	Domestic shipping	1A3d
	International shipping	1C2

207 [a] Detailed source profiles assigned to sources within each subsector are summarized in Table S1.

208 [b] Reference report: https://www.ipcc.ch/report/ar6/wg3/downloads/report/IPCC_AR6_WGIII_FOD_AnnexII.pdf

209

2.3 Components of regional emission inventory

REASv3 for Asia.

212 We used anthropogenic emissions from REASv3.3 developed by ACAP (Asia Center for Air
213 Pollution Research) and NIES (National Institute for Environmental Studies) to fill the gaps
214 where local inventories are not available. REASv3 was developed as a long historical emission
215 inventory for Asia from 1950 - 2015 with monthly variations and relatively high spatial
216 resolution (0.25 degree). Compared to previous versions, REASv3 updated the emission factors
217 and information on control policies to reflect the effect of emission control measures, especially

218 for East Asia. Large power plants are treated as point sources and assigned with coordinates of
219 locations. In REASv3, power plants constructed after 2008 with generation capacity larger than
220 300 MW are added as point sources. Additionally, REASv3 updated the spatial and temporal
221 allocation factors for the areal sources. Emissions of Japan, the Republic of Korea and Taiwan
222 are originally estimated in the system. The REASv3 data were further developed to 2017
223 following the same methodology as Kurokawa et al. (2020) and updated to a finer spatial
224 resolution of 0.1 degree except for NH_3 emissions from fertilizer application where grid
225 allocation factor for 0.1 degree were prepared from that of 0.25 degree for REASv3.2.1 assuming
226 homogeneous distribution of emissions in each 0.25-degree grid cell. We used the REAS
227 estimates for Taiwan directly and replaced REAS with local inventories as illustrated below.

228

MEICv2 for China.

230 For China, we used the anthropogenic emissions from the MEIC model developed and
231 maintained by Tsinghua University. MEIC uses a technology-based methodology to quantify air
232 pollutants and CO_2 from more than 700 emitting sources since 1990 (Li et al., 2017b).
233 Specifically, MEIC has developed a unit-based power plant database, a comprehensive vehicle
234 modeling approach and a profile-based NMVOC speciation framework. Detailed methodology
235 and data sources can be found in previous MEIC studies (Li et al., 2017b; Liu et al., 2015; Zheng
236 et al., 2014). In version 2.0, iron and steel plants, and cement factories are also treated as point
237 sources, which is important to improve industrial emissions estimation (Zheng et al., 2021).
238 MEIC is an online data platform publicly available to the community for emissions calculation,
239 data processing and data downloading. MEIC delivers monthly emissions at various spatial
240 resolutions and chemical mechanisms as defined by the user. We downloaded the emissions at
241 0.1 degree generated from MEIC v2.0 and aggregated it to five anthropogenic sectors: power,
242 industry, residential, transportation and agriculture. We followed the speciation framework in the
243 MEIC model and applied it to other regions of Asia, as described in detail in Sect. 2.4. MEIC
244 emissions of SAPRC99, SAPRC07 and CB05 were used directly in MIX.

245

PKU-NH_3 for NH_3, China.

247 We replaced MEIC with the high-resolution PKU-NH_3 inventory for NH_3 emissions in China
248 developed by Peking University (Huang et al., 2012b; Kang et al., 2016). PKU-NH_3 uses a
249 process-based model to compile NH_3 emissions with emission factors that vary with ambient
250 temperature, soil property, and the method and rate of fertilizer application (Huang et al., 2012b).
251 Compared to the previous version used in MIXv1, PKU-NH_3 further refined emission factors by
252 adding the effects of wind speed and in-field experimental data of NH_3 flux in northern China
253 cropland. Emissions are allocated to 1km × 1km grids using spatial proxies derived from a land
254 cover dataset, rural population, etc (Huang et al., 2012b). Monthly emissions over China,
255 including Hong Kong, Macao, and Taiwan are available from 1980 to 2017. We aggregated the 9
256 sub-sectors into 5 MIX anthropogenic sectors (power, industry, residential, transportation,
257 agriculture) and excluded the agricultural in-field waste burning.

10

258

ANL-India for power plants, India.

ANL-India is a continuously-updated long-term power plant emission inventory for India developed on a unit and monthly basis by Argonne National Laboratory (Lu and Streets, 2012; Lu et al., 2011). Emissions are calculated for more than 1300 units in over 300 thermal power plants based on the detailed information collected from various reports of the Central Electricity Authority (CEA) in India. As much as possible, the accurate and actual operational data of power units/plants are used in inventory development, including geographical locations, capacity, commissioning and retirement time, actual monthly power generation, emission control application, fuel type, source, specifications, and consumption, etc. Detailed method can be found in Lu et al. (2011) and Lu and Streets (2012). ANL-India is available for NO_x, SO_2 and CO_2. In this work, the 2010-2017 period of ANL-India at the monthly level is used directly in MIX. We further merged ANL-India with REASv3 for other species to complete the emission estimation in India. CO_2 emissions of ANL-India at $0.1° \times 0.1°$ grids were used to develop spatial proxies by sectors, year, and month. Then, REASv3 emissions of all other species were re-allocated to grids based on ANL derived spatial proxies. Although ANL-India provides emissions by fuel type, the fuel heterogeneity of thermal power plants is not considered in the re-gridding process of MIX here because about 93% of the thermal power generation in India during 2010-2017 were fueled with coal (Lu and Streets, 2012).

277

JPN (PM2.5EI and J-STREAM) for Japan.

We used the JPN inventory to override the Japan emissions of REAS. JPN was jointly developed by the Ministry of Environment, Japan (MOE-J) for mobile source emissions (i.e., PM2.5 EI) and by the National Institute of Environmental Studies (NIES) for stationary source emissions (J-STREAM). Major anthropogenic sources are included in PM2.5EI, with vehicle emissions explicitly estimated in detail (Shibata and Morikawa, 2021). Emission factors are assigned as a function of average vehicle velocity by 13 vehicle types and regulation years. The hourly average vehicle type of trunk roads and narrow roads are obtained from in-situ measurements. In addition to the running emission exhaust, emissions from engine starting, evaporation, tire ware, road dust and off-road engines are also estimated. To keep consistency with the sector definition of MIX, we excluded the road dust aerosol emissions and mapped other sources to five anthropogenic sectors. For stationary sources, Japan emissions are derived from the Japan's Study for Reference Air Quality Modeling (J-STREAM) model intercomparison project (Chatani et al., 2020; Chatani et al., 2018). Long-term emissions of over 100,000 large stationary sources are estimated based on energy consumption and emission factors derived from the emission reports submitted to the government every three years (Chatani et al., 2020). NMVOC emissions are speciated into SAPRC07 and CB05 using local source profiles. Emissions are distributed to 1km × 1km grids with monthly variations based on spatial and temporal proxies. We re-sampled the monthly JPN emissions to $0.1° \times 0.1°$ grids and merged them into MIXv2.

297

CAPSS for the Republic of Korea.

For the Republic of Korea, we use the official emissions from CAPSS developed by the National Institute of Environmental Research Center (Lee et al., 2011). CAPSS estimated the annual emissions of air pollutants of CO, NO_x, SO_x, PM_{10}, $PM_{2.5}$, BC, NMVOCs and NH_3 based on the statistical data collected from 150 domestic institutions since 1990s (Crippa et al., 2023). There are inconsistencies on the long-term emissions trend of CAPSS due to data and methodology changes over the time. We used the re-analyzed data of CAPSS during 2010-2017, which updated the emission factors and added the missing sources. Point sources, area sources, and mobile sources were processed using source-based spatial allocation methods (Lee et al., 2011). Monthly variations by sectors are derived from REASv3 for the Republic of Korea and were further applied to CAPSS. In MIXv2, the monthly gridded emissions allocated at 0.1-degree grids for the anthropogenic sector (power, industry, residential, transportation, agriculture) of CAPSS are integrated.

GFEDv4s for open biomass burning, Asia.

Emissions over Asia from GFEDv4s database with small fires were used as the default inventory for open biomass burning sources. GFED quantified global fire emissions patterns based on the Carnegie-Ames-Stanford Approach (CASA) biogeochemical model from 1997 onwards (van der Werf et al., 2017). Compared to previous versions, higher quality input datasets from different satellite and in situ data streams are used, and better parameterizations of fuel consumption and burning processes are developed. We calculated emissions for trace gases, aerosol species and CO_2 based on the burned biomass and updated emission factors by vegetation types provided by the GFED dataset (Akagi et al., 2011; Andreae and Merlet, 2001). Monthly and daily emissions were re-gridded from 0.25° to 0.1° and cropped to a unified domain as anthropogenic emissions. Open fires of grassland, shrubland, savanna, forest, and agricultural waste burning are included. We assigned profiles for each source category as listed in Table S1. Model-ready emissions of SAPRC99, SAPRC07 and CB05 were lumped from individual species as described in Sect. 2.4. GFED emissions are further replaced by PKU-Biomass over China.

PKU-Biomass for biomass burning, China.

China's emissions estimated by the PKU-Biomass inventory were used to override GFED emissions for open biomass burning in MIXv2. PKU-Biomass is developed by Peking University based on the MODIS fire radiative energy data for China from 1980 to 2017 (Huang et al., 2012a; Song et al., 2009; Yin et al., 2019). Emission factors of both air pollutants and CO_2 are assigned for four types of biomass burning types including forest, grassland, shrubland fires and agricultural waste burning. PKU-Biomass takes account of the farming system and crop types in different temperate zones. High-resolution emissions (1km) with daily variations are available. We re-gridded emissions to 0.1° × 0.1° and aggregated the emissions to the "open biomass burning" sector. An explicit source profile assignment approach was assigned to each vegetation

337 type. Emissions of three chemical mechanisms were further developed for PKU-Biomass and
338 merged into the MIXv2 final dataset over Asia.

339

EDGARv6 for shipping, Asia.

341 We used the shipping (domestic and international) emissions over Asia derived from EDGARv6
342 in MIXv2. EDGAR is a globally consistent emission inventory for anthropogenic sources
343 developed by the Joint Research Centre of the European Commission (Crippa et al., 2018;
344 Janssens-Maenhout et al., 2019). Emissions of both air pollutants and greenhouse gases are
345 estimated. EDGAR uses international statistics as activity data and emission factors varying with
346 pollutants, sector, technology, and abatement measures for emissions calculation for 1970-2018.
347 Shipping route data are used as spatial proxies to distribute emission estimates to 0.1-degree
348 grids. We downloaded the emissions data for both inland and international shipping from 2010 to
349 2017, processed the data to the MIX domain and aggregated them to the "Shipping" sector.
350 Monthly emissions are only available for 2018. We applied the monthly variations of air
351 pollutants in 2018 to emissions of 2010-2017 accordingly.

352

2.4 NMVOC speciation

354 NMVOC speciation has substantial impacts on the model-ready emissions accuracy and
355 performance of chemical transport models (Li et al., 2014). Selection of profiles turns out to be
356 the most important contributor to uncertainties in emissions of individual species. To reduce the
357 uncertainties due to the inaccurate species mapping, Li et al. (2014) developed an explicit
358 assignment approach based on multiple profiles and mechanism-dependent mapping tables.

359 We processed the gas-phase speciation for NMVOCs following the profile-based mapping
360 procedure, as shown in Fig. 2. The speciation was conducted at a detailed source basis. Firstly,
361 we developed the composite source profile database by combining the US EPA's SPECIATE
362 database v4.5 (last access: June 2019) (Simon et al., 2010) and available local measurements
363 (e.g., (Akagi et al., 2011; Mo et al., 2016; Xiao et al., 2018; Yuan et al., 2010). The complete list
364 of source profiles used in this work is provided in Table S1. To diminish the uncertainties due to
365 inappropriate sampling and analyses techniques regarding Oxygenated Volatile Organic
366 Compounds (OVOCs), we applied the OVOC correction to those incomplete profiles. The
367 detailed method can be found in previous studies (Li et al., 2014). Especially, the following
368 sources have significant OVOC emitted which should be addressed: coal combustion in
369 residential stoves (31%), residential wood and crop residue fuel use (23% ~ 33%) and diesel
370 engines (28% ~ 47%). Secondly, we assigned the composite profile database to each component
371 inventory to develop emissions of individual species. Lastly, individual species were lumped to
372 three chemical mechanisms (SAPRC99, SAPRC07, CB05) based on the conversion factors
373 derived from mechanism-dependent mapping tables (Carter, 2015).

374 For the Republic of Korea and Hong Kong, we applied the speciation factor for SAPRC99 and
375 CB05 by sectors developed from the SMOKE-Asia model, which have been used for MIXv1

376 (Woo et al., 2012). Emissions of SAPRC07 were further developed from SAPRC99 based on
377 Table S2, which applied MEIC speciated results.
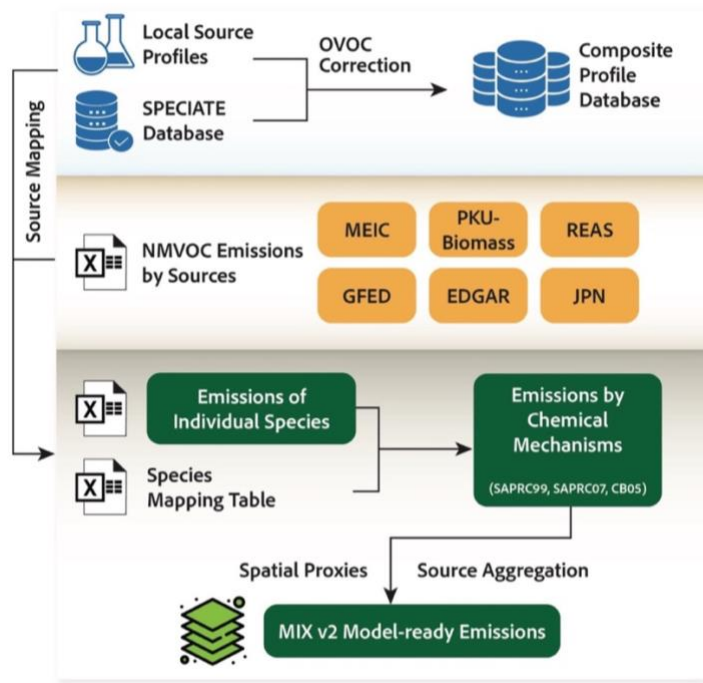
378
379   **Figure 2. NMVOC speciation scheme used in MIXv2.**

380

381 **2.5 Limitations and Uncertainties**

382 As a mosaic inventory, MIXv2 has several limitations when integrating various gridded products
383 into a unified dataset. Firstly, inconsistencies could exist at country boundaries where different
384 datasets were used for the adjacent countries (Janssens-Maenhout et al., 2015), for example, the
385 border between China and India. But limited effects are anticipated here given the small area
386 affected due to the high spatial resolution and the low population density at the border. Secondly,
387 extracting emissions by country from gridded maps may introduce uncertainties especially for
388 power plants located near the coast. This issue is more important because gridded emissions are
389 developed with higher spatial resolutions than earlier versions. Using an extended country map
390 by assigning extra adjacent grids of "ocean" with the neighboring country can reduce this bias.
391 We also acknowledge the general inconsistency of uncertainty levels between countries where
392 different inventories are used following various data sources and approaches. For air quality
393 simulation purposes, the lack of diurnal variations and vertical distribution is another limitation
394 when applying MIXv2 data directly. Development of Asia-specific temporal and vertical profiles
395 is important to improve the model simulation performance in the future.

396 It's always difficult to quantify the uncertainties for a mosaic emission inventory such as MIXv2.
397 The uncertainties for each of the component inventories are discussed in detail in corresponding

398　studies (Kang et al., 2016; Kurokawa and Ohara, 2020; Yin et al., 2019; Zheng et al., 2018).
399　Here we summarized the uncertainty estimation by Asian regions in previous studies in Table 3.
400　The uncertainty ranges are quantified based on propagation of uncertainty (Kurokawa and Ohara,
401　2020; Lei et al., 2011; Zhang et al., 2009) or thousands of Monte Carlo simulations (Lu et al.,
402　2011; Paliwal et al., 2016; Shan et al., 2020; Shi and Yamaguchi, 2014; Sun et al., 2018; Zhao et
403　al., 2011; Zhao et al., 2012; Zhao et al., 2013; Zhou et al., 2017).

404　In regard of anthropogenic sectors, the precision of emission estimates for SO_2, NO_x, and CO_2 is
405　higher than that of other pollutants, owing to the minimal uncertainties associated with power
406　plants and large industrial facilities. This is particularly notable in the case of MIXv2, where
407　uncertainties are even lower due to the integration of unit-based power plant information for both
408　China and India. While uncertainties for CO and NMVOC are comparable, they are higher than
409　those for SO_2, NO_x, and CO_2, because of substantial emission contributions from biofuel
410　combustion. Emissions for particulate matter (especially BC and OC) tend to be more uncertain
411　compared to trace gases, primarily due to the low data availability of accurate activity rates and
412　emission factors related to residential biofuel combustion. The need for more detailed
413　information at the technology or facility level in regions, such as India, OSA, and SEA, is crucial
414　to narrow down the overall uncertainties in Asia in the future. For open biomass burning,
415　previous investigations have estimated low uncertainty ranges for species like CO, NMVOC, and
416　OC, while more further analyses are in urgent need. In this work, we conducted uncertainty
417　analyses qualitatively by comparing the MIXv2 estimates with other bottom-up inventories and
418　those derived from satellite retrievals in Sect. 4 (Li et al., 2018). In short summary, generally
419　consistent emission estimates and trends over Asia are found based on bottom-up and top-down
420　comparisons in Sect. 4. Discrepancies persist, especially in regions like South Asia and Southeast
421　Asia, as well as among species like BC and NMVOC.

422

423 **Table 3. Uncertainties in emission estimates by Asian regions (95% confidence intervals if not noted; unit: %)**

Regions, Anthropogenic or Open Biomass	NO_x	SO_2	NO_x	CO	NMVOC	NH_3	PM_{10}	$PM_{2.5}$	BC	OC	CO_2	Year	Reference
							±91	±107	±187	±229		2005	Lei et al. (2011)
	-13~37	-14~13	-13~37				-14~45	-17~54	-25~136	-40~121		2005	Zhao et al. (2011)
				-20~45								2005	Zhao et al. (2012)
	±31	±12	±31	±70	±68		±132	±130	±208	±258		2006	Zhang et al. (2009)
		-16~17							-41~80	-44~92		2010	Lu et al. (2011)
China, Anthropogenic	-15~35	-15~26	-15~35	-18~42			-15~54	-15~63	-28~126	-42~114		2010	Zhao et al. (2013)
	±35	±40	±35	±73	±76	±82	±83	±94	±111	±193	±19	2015	Kurokawa et al. (2020)
	-26~34	-22~25	-26~34	-31~41								2015	Sun et al. (2018)
					-32~56	-14~13						2015	Zhang et al. (2017)
											-15~30	2017	Shan et al. (2020)*
		-15~16							-41~87	-44~92		2010	Lu et al. (2011)
India, Anthropogenic	±35	±41	±35	±136	±115	±111	±120	±151	±133	±233	±27	2015	Kurokawa et al. (2020)
									±33			2011	Paliwal et al. (2016)
Japan, Anthropogenic	±32	±34	±32	±45	±63	±103	±68	±74	±58	±100	±13	2015	Kurokawa et al. (2020)
OEA, Anthropogenic	±60	±38	±60	±67	±63	±94	±69	±85	±82	±168	±19	2015	Kurokawa et al. (2020)
OSA, Anthropogenic	±34	±40	±34	±87	±73	±93	±96	±112	±124	±211	±19	2015	Kurokawa et al. (2020)
SEA, Anthropogenic	±38	±46	±38	±124	±86	±115	±125	±155	±161	±232	±25	2015	Kurokawa et al. (2020)
China, Biomass	-37~37	-54~54	-37~37	-4~4	-9~9	-49~48	-7~6	-13~1	-61~61	-20~19	-3~3	2012	Zhou et al. (2017)
SEA, Biomass	±23	±30	±23	±20	±18	±10			±20	±31	±15	2010	Shi and Yamaguchi (2014)

424 * 97% Confidence Interval

426   **Table 4. Anthropogenic | Open biomass[a] emissions of MIXv2 by Asian countries and regions in 2017.**

Country	NO$_x$[b]	SO$_2$	CO	NMVOC	NH$_3$	PM$_{10}$	PM$_{2.5}$	BC	OC	CO$_2$[b]
China[c]	**22.37 | 0.22**	**10.62 | 0.02**	**137.02 | 4.40**	**29.36 | 1.66**	**9.18 | 0.08**	**10.20 | 0.41**	**7.65 | 0.35**	**1.26 | 0.03**	**2.09 | 0.17**	**11.34 | 0.07**
Japan	1127.0 | 8.4	274.8 | 1.5	2543.1 | 192.0	927.1 | 141.2	397.7 | 2.9	84.3 | 30.1	40.7 | 19.6	14.9 | 1.3	7.5 | 11.9	785.9 | 3.4
Korea, DPR	194.6 | 3.5	83.8 | 0.7	2580.5 | 92.7	140.4 | 61.7	107.4 | 1.6	96.6 | 13.5	52.6 | 9.3	10.0 | 0.6	16.4 | 5.4	29.7 | 1.5
Korea, Republic of	979.1 | 2.8	266.7 | 0.5	522.1 | 61.0	917.1 | 44.5	292.5 | 0.9	127.6 | 9.5	64.5 | 6.2	11.2 | 0.4	31.3 | 3.7	581.9 | 1.1
Mongolia	125.5 | 28.3	124.9 | 7.8	1057.9 | 945.5	50.3 | 368.7	196.1 | 17.6	45.5 | 129.7	20.6 | 110.3	2.7 | 4.2	3.5 | 62.7	18.3 | 14.2
Other East Asia[c,d]	**2.43 | 0.04**	**0.75 | 0.01**	**6.70 | 1.29**	**2.03 | 0.62**	**0.99 | 0.02**	**0.35 | 0.18**	**0.18 | 0.15**	**0.04 | 0.01**	**0.06 | 0.08**	**1.42 | 0.02**
India[c]	**9.34 | 0.11**	**13.82 | 0.01**	**61.23 | 1.91**	**14.46 | 1.23**	**9.87 | 0.03**	**7.20 | 0.27**	**4.97 | 0.18**	**0.86 | 0.01**	**1.72 | 0.09**	**2.88 | 0.04**
Afghanistan	83.2 | 0.2	45.0 | 0.0	560.2 | 2.7	131.2 | 1.4	320.3 | 0.0	39.9 | 0.4	30.7 | 0.3	8.3 | 0.0	12.1 | 0.1	11.1 | 0.1
Bangladesh	342.3 | 2.8	224.5 | 0.3	3074.5 | 41.9	836.0 | 15.7	922.5 | 0.5	685.6 | 5.8	350.1 | 4.4	43.6 | 0.2	114.3 | 2.0	127.7 | 0.9
Bhutan	0.8 | 1.0	0.5 | 0.4	31.5 | 30.0	6.4 | 14.8	2.8 | 0.3	13.6 | 5.9	5.1 | 4.3	0.4 | 0.2	1.2 | 3.1	0.8 | 0.6
Maldives	0.6 | 0.0	0.3 | 0.0	1.3 | 0.0	0.5 | 0.0	0.0 | 0.0	0.0 | 0.0	0.0 | 0.0	0.0 | 0.0	0.0 | 0.0	0.1 | 0.0
Nepal	70.6 | 7.0	61.2 | 2.2	2143.1 | 189.7	483.5 | 94.9	263.8 | 1.9	238.0 | 36.5	159.6 | 26.5	24.3 | 1.1	79.1 | 19.1	42.8 | 3.6
Pakistan	638.7 | 6.7	1607.7 | 0.6	9000.4 | 133.3	2134.7 | 126.9	1890.5 | 2.7	1479.4 | 16.5	914.0 | 8.9	108.6 | 1.0	327.6 | 3.3	308.8 | 2.2
Sri Lanka	205.0 | 2.2	84.7 | 0.2	1356.4 | 31.2	390.7 | 21.3	99.6 | 0.5	144.5 | 4.0	101.0 | 2.8	19.0 | 0.2	46.8 | 1.0	39.5 | 0.7
Other South Asia[c,e]	**1.34 | 0.02**	**2.02 | 0.00**	**16.17 | 0.43**	**3.98 | 0.27**	**3.50 | 0.01**	**2.60 | 0.07**	**1.56 | 0.05**	**0.20 | 0.00**	**0.58 | 0.03**	**0.53 | 0.01**
Brunei	9.4 | 0.1	2.7 | 0.0	24.8 | 1.9	26.5 | 0.4	1.4 | 0.0	4.6 | 0.2	1.7 | 0.1	0.1 | 0.0	0.1 | 0.1	4.3 | 0.0
Cambodia	74.2 | 189.7	78.7 | 16.7	1155.5 | 2899.1	230.1 | 943.7	85.2 | 34.2	170.0 | 397.9	87.9 | 301.7	9.8 | 16.7	33.3 | 133.5	26.3 | 62.7
Indonesia	2560.0 | 86.3	3260.5 | 9.2	16039.6 | 2439.6	5438.5 | 559.2	1848.0 | 26.4	1258.0 | 264.6	839.1 | 188.3	136.5 | 8.9	338.5 | 97.1	619.0 | 36.6
Laos	61.4 | 115.8	126.2 | 10.0	296.3 | 1641.4	55.5 | 569.9	69.5 | 18.4	93.7 | 224.4	39.7 | 173.2	3.2 | 9.5	9.2 | 74.0	20.0 | 36.9

Region										
Malaysia	224.7 | 3.0	13.7 | 6.6	14.4 | 0.9	137.0 | 14.5	226.7 | 20.5	237.2 | 2.1	1029.2 | 65.9	1234.6 | 167.2	250.3 | 0.8	627.1 | 8.6
Myanmar	68.3 | 78.0	104.2 | 182.8	32.3 | 20.7	206.2 | 387.9	292.3 | 510.1	679.1 | 40.6	936.1 | 1280.0	3168.3 | 3576.8	315.9 | 23.4	185.5 | 233.3
Philippines	159.0 | 3.0	61.4 | 4.7	39.7 | 0.9	197.5 | 12.7	315.8 | 18.0	469.9 | 1.9	1031.0 | 91.8	3705.7 | 139.1	974.2 | 0.8	881.4 | 10.1
Singapore	44.7 | 0.0	0.3 | 0.0	0.9 | 0.0	60.8 | 0.0	77.0 | 0.0	4.4 | 0.0	286.8 | 0.1	55.4 | 0.1	74.8 | 0.0	78.0 | 0.0
Thailand	328.2 | 22.6	119.5 | 39.9	45.5 | 6.6	367.1 | 99.7	522.8 | 139.3	631.0 | 14.3	1546.1 | 585.4	5073.4 | 1056.3	337.3 | 6.1	1081.5 | 72.7
Vietnam	274.5 | 13.9	143.0 | 25.3	54.3 | 4.2	390.1 | 62.2	671.9 | 87.7	734.0 | 9.2	1335.1 | 364.1	6224.7 | 664.2	517.0 | 3.7	546.8 | 44.1
Southeast Asia[c]	**1.77 | 0.26**	**0.82 | 0.56**	**0.34 | 0.07**	**2.33 | 1.24**	**3.63 | 1.66**	**4.76 | 0.15**	**11.91 | 4.46**	**36.98 | 12.59**	**5.94 | 0.07**	**6.11 | 0.76**
Asia (2017)[c]	**17.95 | 0.40**	**5.28 | 0.93**	**2.71 | 0.12**	**16.69 | 1.97**	**24.00 | 2.59**	**28.32 | 0.29**	**61.79 | 8.24**	**258.22 | 20.61**	**33.16 | 0.12**	**41.61 | 1.15**
Asia (2010/2017)[f]	**0.86 | 1.58**	**1.25 | 1.64**	**1.17 | 1.52**	**1.23 | 1.61**	**1.21 | 1.61**	0.96 | 1.39	0.89 | 1.36	**1.20 | 1.49**	**1.32 | 1.55**	**1.04 | 1.56**
Asia (2011/2017)	**0.93 | 1.55**	**1.26 | 1.74**	**1.19 | 1.30**	**1.25 | 1.60**	**1.23 | 1.64**	0.96 | 1.52	0.92 | 1.29	**1.18 | 1.88**	**1.39 | 1.45**	**1.10 | 1.33**
Asia (2012/2017)	**0.96 | 1.88**	**1.25 | 2.16**	**1.19 | 1.62**	**1.24 | 1.98**	**1.23 | 2.02**	0.98 | 1.87	0.95 | 1.62	**1.17 | 2.22**	**1.39 | 1.86**	**1.12 | 1.65**
Asia (2013/2017)	**0.96 | 1.67**	**1.21 | 1.87**	**1.17 | 1.53**	**1.21 | 1.74**	**1.19 | 1.78**	1.00 | 1.65	0.96 | 1.42	**1.15 | 1.89**	**1.32 | 1.59**	**1.09 | 1.49**
Asia (2014/2017)	**0.97 | 3.15**	**1.16 | 3.72**	**1.11 | 2.45**	**1.14 | 3.31**	**1.13 | 3.44**	1.00 | 3.17	0.98 | 2.39	**1.10 | 4.18**	**1.21 | 2.85**	**1.04 | 2.51**
Asia (2015/2017)	**0.97 | 4.25**	**1.09 | 5.22**	**1.05 | 2.85**	**1.07 | 4.49**	**1.05 | 4.73**	1.01 | 4.46	0.97 | 3.08	**1.06 | 6.36**	**1.12 | 3.72**	**1.01 | 3.05**
Asia (2016/2017)	**0.97 | 1.31**	**1.04 | 1.35**	**1.01 | 1.27**	**1.01 | 1.32**	**1.00 | 1.36**	1.01 | 1.25	0.98 | 1.27	**1.01 | 1.32**	**1.05 | 1.28**	**0.99 | 1.28**

427   [a] Anthropogenic includes power, industry, residential, transportation and agriculture. Open biomass represents the "Open Biomass Burning" sector.

428   [b] Tg yr^{-1} for CO_2, Gg yr^{-1} for other species.

429   [c] Bold values are with the following units: Pg yr^{-1} for CO_2, Tg yr^{-1} for other species.

430   [d] Other East Asia represents East Asia other than China.

431   [e] Other South Asia represents South Asia other than India.

432   [f] Asia (year/2017) represents the ratio of emissions (year) to emissions (2017) for all of Asia within the MIXv2 domain. The detailed emissions for 2010-2017 by
433   countries and sectors are summarized in Table S3.

434

435

3. Results and Discussions

3.1 Asian emissions in 2017

In 2017, MIXv2 estimated emissions of Asia as follows: 41.6 Tg NO_x, 33.2 Tg SO_2, 258.2 Tg CO, 61.8 Tg NMVOC, 28.3 Tg NH_3, 24.0 Tg PM_{10}, 16.7 Tg $PM_{2.5}$, 2.7 Tg BC, 5.3 Tg OC, and 18.0 Pg CO_2 for all anthropogenic sources including power, industry, residential, transportation and agriculture. Emissions are summarized by Asian regions, including China, East Asia Other than China (OEA), India, South Asia other than India (OSA) and Southeast Asia (SEA), as shown in Table 4 and Table S3. China, India, and SEA together account for > 90% of the total Asian emissions. China dominates the emissions (> 50%) of CO_2 (11.3 Pg, 63%), NO_x (22.4 Tg, 54%), and CO (137.0 Tg, 53%), and contributes more than 30% to all other species. The contributions of India are larger than 30% for SO_2 (13.8 Tg, 42%), NH_3 (9.8 Tg, 35%), BC (0.86 Tg, 32%), OC (1.7 Tg, 33%), PM_{10} (7.2 Tg, 30%), and $PM_{2.5}$ (5.0 Tg, 30%). SEA ranks 3rd for all species, including CO_2 (1.8 Pg, 10%), NO_x (6.1 Tg, 15%), SO_2 (5.9 Tg, 18%), NMVOC (11.9 Tg, 19%), NH_3 (4.8 Tg, 17%), and ~15% of aerosol species. OEA's share varies from 1% (aerosol species) to 8% (CO_2). Emission proportions of OSA are around 11% for NH_3, OC, and PM_{10}, and less than 10% for others.

Sectoral contribution varies among species in Asia, according to our estimates. Power plants contribute significantly to SO_2 (1st contributor, 38%) and CO_2 (2nd contributor, 33%). Industry dominates the emissions of CO_2 (41%), NMVOC (44%), $PM_{2.5}$ (39%), and PM_{10} (47%). For NO_x, transportation accounts for 33% of the total emissions, followed by industry (24%) and inland and international shipping (18%). The residential sector contributes > 38% of emissions for $PM_{2.5}$, BC, CO, and OC. NH_3 is dominated by agriculture (81%), followed by 13% from residential.

Open biomass burning plays a key role in SEA and OEA's emissions budget, and is a minor contributor for other regions, as shown in Table 4 and Figure 3. Including the open biomass burning sector increases the emissions of OC, $PM_{2.5}$, PM_{10}, NMVOC, CO and CO_2, by 69%, 53%, 46%, 37%, 34% and 15%, respectively for SEA. Due to the active fire events, Southeast Asia is the largest emission contributor for OC, PM_{10}, $PM_{2.5}$ and NMVOC in 2014 and 2015. Additionally, OEA has a significant emission increment for NMVOC (30%), OC (143%), PM_{10} (52%) and $PM_{2.5}$ (81%) when taking biomass burning into account. Given the large contributions to ozone and climate change from NMVOC, CO and aerosols, it's important to address the open biomass burning contributions in designing mitigation strategies for these areas.

In a global context, Asia shares out 43%~56% of the global anthropogenic emissions in 2017, including 44% for NO_x, 43% for SO_2, 49% for CO_2, 51% for NH_3, 55% for CO, 50% for NMVOC, and over 50% for all PM species. Emissions over Asia are derived from MIXv2, and emissions over the rest of the world are estimated by EDGARv6. Figure S1 depicts the emissions trend by Asian regions, United States and OECD-Europe from anthropogenic sources. Asia is playing a more and more important role in global climate change as its CO_2 emission fraction has

474   increased by 7% during 2010-2017. Especially, with the general emission reductions in the U.S.
475   and OECD-Europe, India and Southeast Asia is catching up with the emissions of these two
476   developed regions for NO_x, SO_2 and CO_2, and already surpassed their emissions for other
477   species. As of now, U.S. and OECD-Europe emissions are in general comparable to those of
478   OSA for most air pollutants.

479

3.2 Emissions evolution from 2010–2017

For anthropogenic sources, driven by stringent air pollution control measures implemented over China and OEA since 2010, Asian emissions have declined rapidly by 24.3% for SO_2, 16.6% for CO, 17.2% for PM_{10}, 18.7% for $PM_{2.5}$, 14.2% for BC and 19.8% for OC, according to our estimates. On the contrary, CO_2, NMVOC and NH_3 still show emissions increasing continuously, with growth rates of 16.5%, 12.6%, and 4.4% during 2010-2017, respectively. The emissions for 2010-2017 are summarized in Table S3 and shown in Fig. 3 and Fig. 4. As demonstrated in Fig. 4, power, industry, residential and transportation contribute to the rapid emission changes. In contrast to the smoothly changing patterns for anthropogenic, open biomass burning emissions vary from year to year, peaking in 2015 as a result of El Niño (Field et al., 2016). Open fire activities dominate the SEA emission changes for CO, OC, NMVOC, PM_{10} and primary $PM_{2.5}$ (see Fig. 3). Marked reductions are estimated for China, with a concurrent increase over India and Southeast Asia for all species except CO_2, NMVOC and NH_3 (see Fig. 5). Consequently, air pollutants, including ozone and secondary aerosol precursors of NO_x, have shifted southward (Zhang et al., 2016). This changing spatial pattern has been confirmed from observations as described in previous studies (Samset et al., 2019). We illustrate the driving forces of emissions evolution for each species below. Shipping is not included in the following analyses.

NO_x. NO_x emissions show increasing-decreasing-increasing trend for 2010-2017, with a peak in 2012. This trend is a combination of significant power plant emissions reduction (-22% from 2010-2017), and emissions increase from industry (+4%) and transportation (+6%). As estimated, China's emissions for all anthropogenic sectors dropped by 4.6 Tg (-17%) from 2010-2017, along with 2.6 Tg (+38%) emissions growth from India and 0.9 Tg (+19%) from SEA. As a result, China's contribution decreased from 63% to 54%, and Indian share grew from 16% to 22% (anthropogenic, Fig. 5a). In China, power plant emissions dropped by 4.5 Tg (-51%) because very stringent emission standards are implemented for power plants since 2003, which has continuous substantial impacts on SO_2, NO_x and particulate matters (Chinese National Standards GB 13223-2003 and 3223-2011) (Zheng et al., 2018). Furthermore, "Ultra-low" emission standards were set up by the Chinese government in 2015 to further reduce emissions from coal-fired power plants by 60% by 2020. OEA shows 21% emissions decrease because of continuous control measures over industry (-16%) and transportation (-32%). Due to insufficient control strategies in India, OSA and SEA, NO_x anthropogenic emissions have grown by 38%, 18% and 19%, respectively, mainly driven by power plants and vehicle growth (see Fig. 5a). Open biomass burning has limited effect (~11%) on NO_x emissions over SEA and is neglectable for other regions (<3%).

SO_2. SO_2 emissions rapidly declined from 43.8 Tg to 33.1 Tg during 2010-2017, peaking in 2012. Significant reductions of industrial SO_2 emissions (-8.7 Tg, -39%) lead to the marked total emissions decrease (see Fig. 4). China's emissions dropped by 62%, partly offset by the concurrent emissions increase of India (+46%) and Southeast Asia (+41%). Stringent control measures shutting down small industrial boilers and cleaning larger ones in China are the primary driving forces (Zheng et al., 2018). New emissions standards were set up for coal-fired industrial boilers with tightened SO_2 limit values (Zheng et al., 2018). In addition, nationwide

521 phasing out of outdated industrial capacity and small, polluting units has been carried out in
522 China since 2013. Consequently, China's emission fraction decreases from 64% to 32%, ranking
523 2nd in 2017. India's proportion grew from 22% to 41%, and nowadays it's the largest SO_2 emitter
524 in Asia (anthropogenic, see Fig. 5b). Relatively small emission changes are estimated for OEA (-
525 0.2 Tg) and OSA (+0.6 Tg). Significant emissions growth from power plants drives the total
526 anthropogenic increase by 44%, and a 41% rise when considering additional open biomass
527 burning for SEA.

528 *CO*. Anthropogenic CO shows moderate emissions reduction (-16%) since 2010, driven by the
529 clean air actions implemented in China covering industry (-38% changes), residential (-20%) and
530 transportation (-22%). Based on the index decomposition analysis, the improvements in
531 combustion efficiency and oxygen blast furnace gas recycling in industrial boilers are the largest
532 contributors to the emission reductions in China (Zheng et al., 2018). Replacing polluted fuel
533 (biofuel, coal) with cleaner fuels (natural gas, electricity) is the primary driving force in the
534 residential sector. Despite the rapid vehicle growth which would typically yield a CO increase,
535 pollution control measures reduced the net CO emission factors by fleet turnover with cleaner
536 models replacing the older, more polluted vehicles in the market. OEA shows emission
537 reductions in industry (-37%), residential (-22%) and transportation (-28%). Residential fuel
538 combustion decreases by 20% and 11% for SEA and India, respectively, having a canceling
539 effect on the total emissions growth for these two regions. Open biomass burning accounts for
540 25% ~ 77% of CO emissions in SEA, which drives the total emissions reduction by 19% in 2017
541 compared to 2010. Additionally, the climate anomaly due to El Niño in 2015 leads to the rapidly
542 CO emissions drop from 2015 to 2016 in SEA.

543 *CO_2*. Driven by economic and population growth, anthropogenic CO_2 emissions show a rapid
544 increasing trend for China (15%), India (32%), OSA (32%) and SEA (21%). We found slight
545 emission decreases for OEA (-2%). Power, industry, and transportation grew by 28%, 12% and
546 35%, respectively, driving the total emissions increase continuously. In contrast, we estimate a
547 5% CO_2 emission reduction from the residential sector, attributed to reduced fuel combustion.
548 Notable emissions have increased for sectors apart from residential for India (increasing rates
549 varying between 39% ~ 57%), OSA (43% ~ 56%), and SEA (9% ~ 48%). Fractions by regions
550 are stable during the studied period, with 62% contribution from China, 8% from OEA, 16%
551 from India, 3% from OSA, and 11% from SEA (see Fig. 3). Open biomass burning curbs the
552 total emission growth in SEA from +21% to +5%.

553 *NMVOC*. Differing from the decreasing emission trend for NO_x, SO_2 and CO, NMVOC
554 increases by 13% for anthropogenic, and 6% for all sources with open biomass burning. In
555 China, the industrial sector (+5.1Tg, +35%) is the major reason for the emissions growth, and
556 industrial solvent use (e.g., architecture paint use, wood paint use) is the largest contributor. The
557 share of solvent use rapidly rises from 28% in 2010 to 42% in 2017. In addition, oil production,
558 distribution and refineries, and chemical production lead to a corresponding emissions increase
559 by 44% (Li et al., 2019b). Due to fuel transfer in residential stoves and the effective pollution
560 control measures for on-road vehicles, China shows 18% and 22% emissions decreases,
561 respectively, slowing down the increasing trend. Industry and transportation drive the
562 anthropogenic emissions in India and SEA growing by 18% and 13%, respectively (see Fig. 5c).

563 In SEA, 64% of the total emissions are contributed by open biomass burning in 2015. Compared
564 to 2010, 2017 total emissions decreased by 12% in SEA, attributed to biomass burning.
565 NMVOCs are speciated into three chemical mechanisms following the source-profile based
566 methodology (see Sect. 2.4). We analyzed the speciation results in Sect. 3.5.

567 *NH$_3$*. As estimated by MIXv2, NH$_3$ emissions are generally flat, with slight increases (+4%) over
568 Asia due to the lack of targeted control measures. Over 80% of the total emissions are
569 contributed by fertilizer application and livestock manure. Transportation emissions in 2017 are
570 2.8 times greater than those in 2010 due to vehicle growth, which can play a key role for urban
571 air quality. India is the largest contributor (35%), followed by China (32%) and SEA (17%) (see
572 Fig. 3). India and OSA emissions show monotonic 7% and 20% increases, respectively.
573 According to our estimates, China decreases by 8% reflecting the agricultural activity rate
574 changes. Limited effects are estimated from open fires over NH$_3$ emissions budget, peaking at
575 19% of the total in 2015 for SEA.

576 *Particulate Matter (PM)*. PM emissions are estimated to have decreased in Asia: -4.9 Tg PM$_{10}$ (-
577 17%), -3.8 Tg PM$_{2.5}$ (-19%), -0.45 Tg BC (-14%), -1.3 Tg OC (-20%) for anthropogenic, and -
578 6.5 Tg PM$_{10}$ (-20%), -5.0 PM$_{2.5}$ (-21%), -0.51 Tg BC (-15%), -1.9 Tg OC (-23%) after including
579 open biomass burning. Industrial and residential sectors are the primary driving forces of the
580 emissions reduction. In China, the strengthened particulates standard for all emission-intensive
581 industrial activities, including iron and steel making, cement, brick, coke, glass, chemicals, and
582 coal boilers have driven the technology renewal and the phasing out of outdated, highly polluting
583 small facilities (Zheng et al., 2018). Pollution control measures reduced power plant emissions
584 by ~30% for PM$_{10}$, PM$_{2.5}$ and BC, and counterbalanced the transportation emissions despite
585 vehicle ownership increasing by 270% in seven years. Other East Asia shows significant
586 anthropogenic emissions reduction for all PM species: -32% for PM$_{10}$, -33% for PM$_{2.5}$, -27% for
587 BC, and -31% for OC. Flat trends are estimated in India for all PM species (±8%). Reduction in
588 biofuel fuel use led to the residential emission reduction of PM in India and SEA. Increasing
589 industrial activities led to 24% - 35% anthropogenic emissions growth for PM$_{10}$ and PM$_{2.5}$ in
590 OSA. As a result, China's emission fractions are shrinking, with growing contributions from
591 India and OSA (see Fig. 5d). Taking PM$_{2.5}$ as an example, the emissions shares among Asian
592 regions have changed significantly between 2010 and 2017: from 58% to 46% for China, 23% to
593 30% for India, and 12% to 14% for SEA (anthropogenic, Fig. 5d). Open biomass burning
594 dominates the SEA emissions changes between 2010-2017: -19% for PM$_{10}$, -24% for PM$_{2.5}$, -
595 20% for BC, and -30% for OC.

596
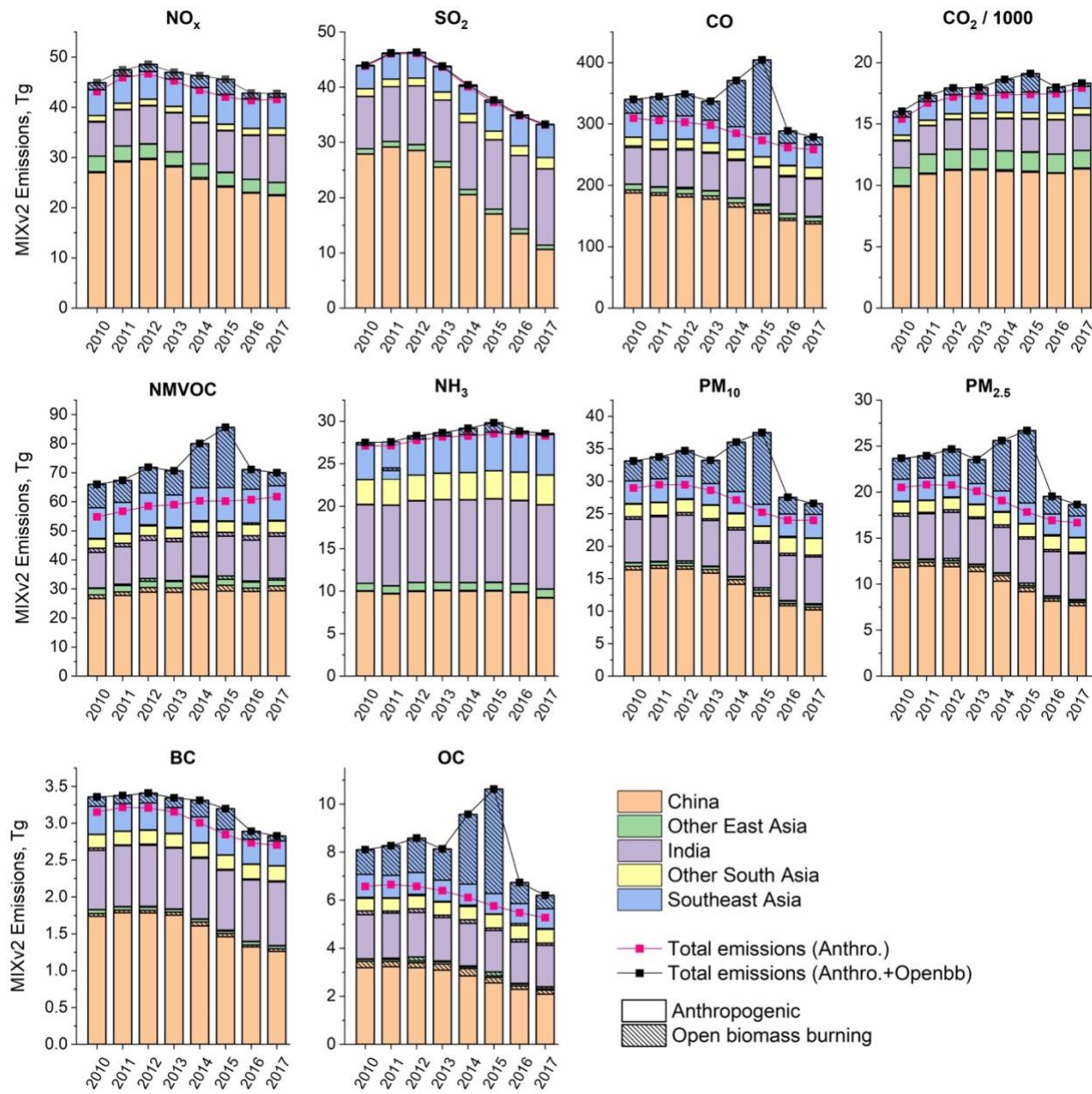
Figure 3. Emission changes by countries / regions from 2010 – 2017. Shares of open biomass burning for each region are shown as shadowed blocks.

24
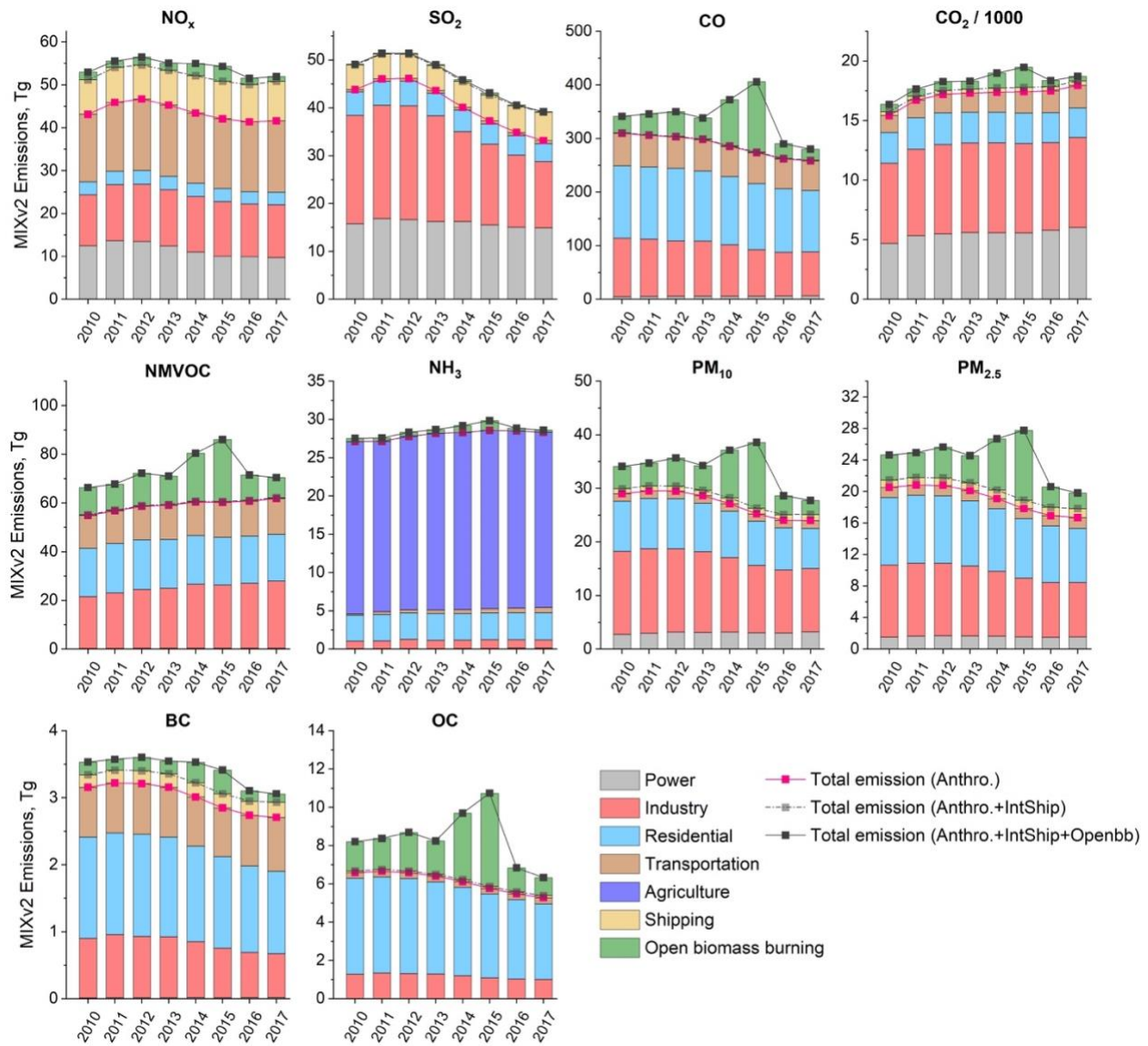
Figure 4. Emission changes by sectors in Asia from 2010 – 2017.

610

611
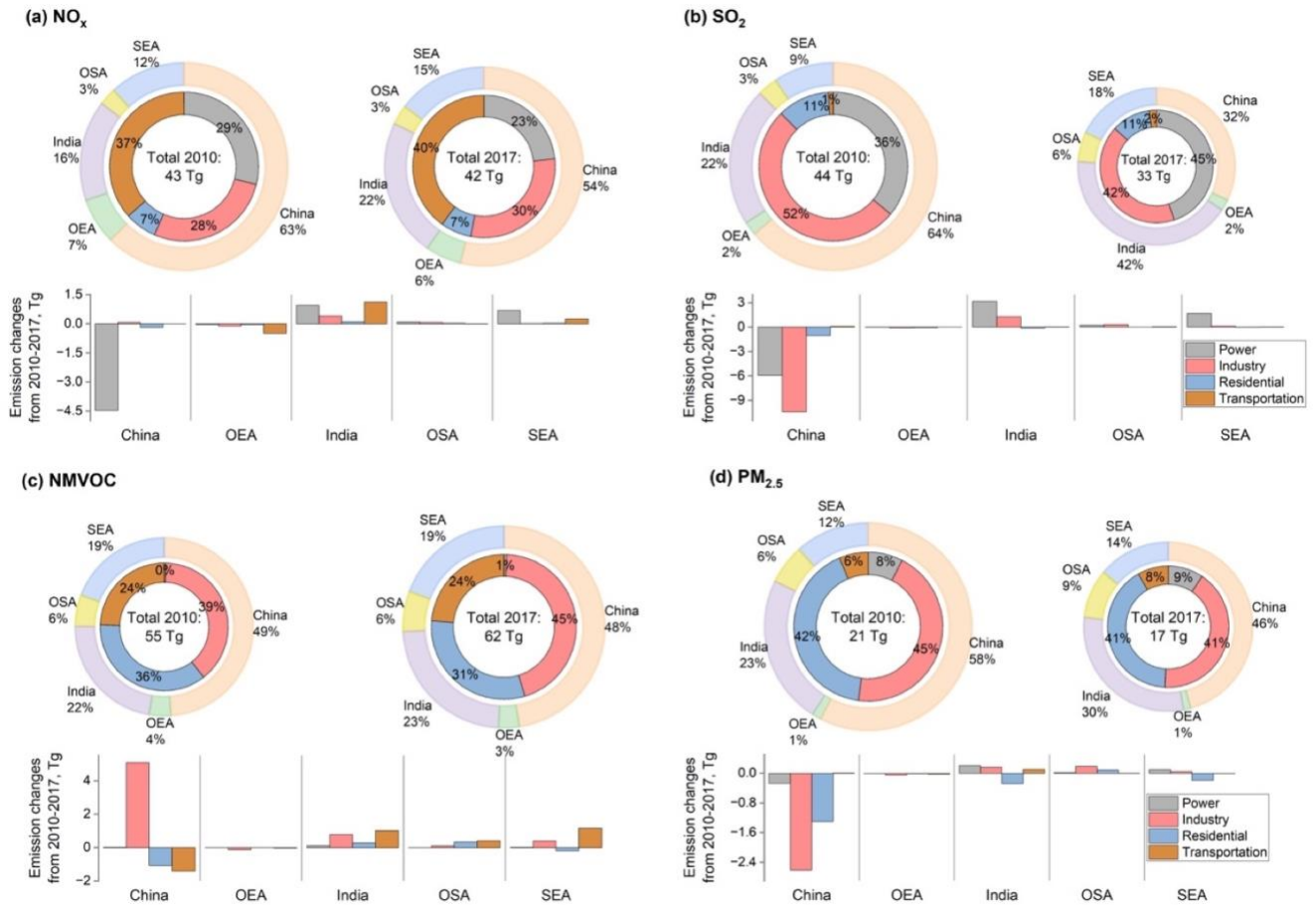
Figure 5. Emission changes for anthropogenic sources (power, industry, residential, and transportation) by regions and sectors from 2010 – 2017 for (a) NO$_x$, (b) SO$_2$, (c) NMVOC and (d) PM$_{2.5}$. The pie sizes are scaled with the total anthropogenic emissions in Asia. The unit for the total emission values in the center is Tg per year. OEA denotes East Asia other than China, OSA represents South Asia other than India, SEA is Southeast Asia.
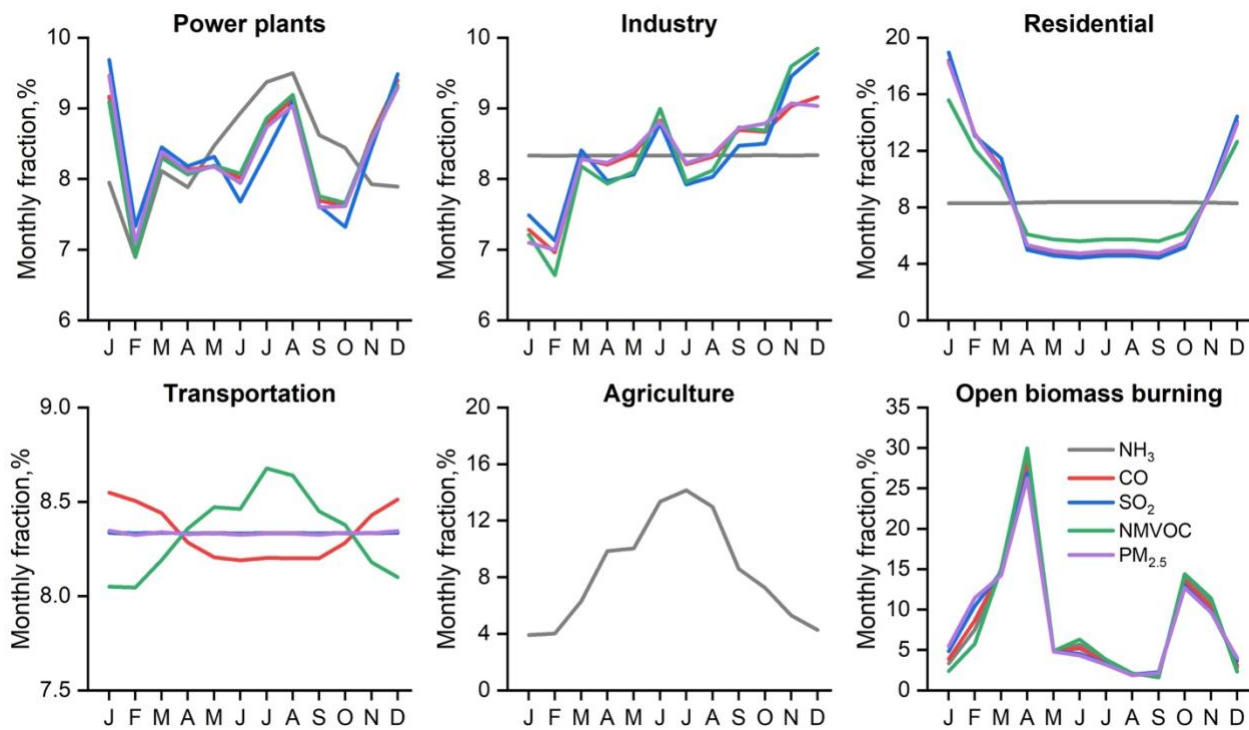
Figure 6. Monthly variations of emissions in Asia by sectors, 2017. For agriculture, only NH₃ emissions are estimated.

620
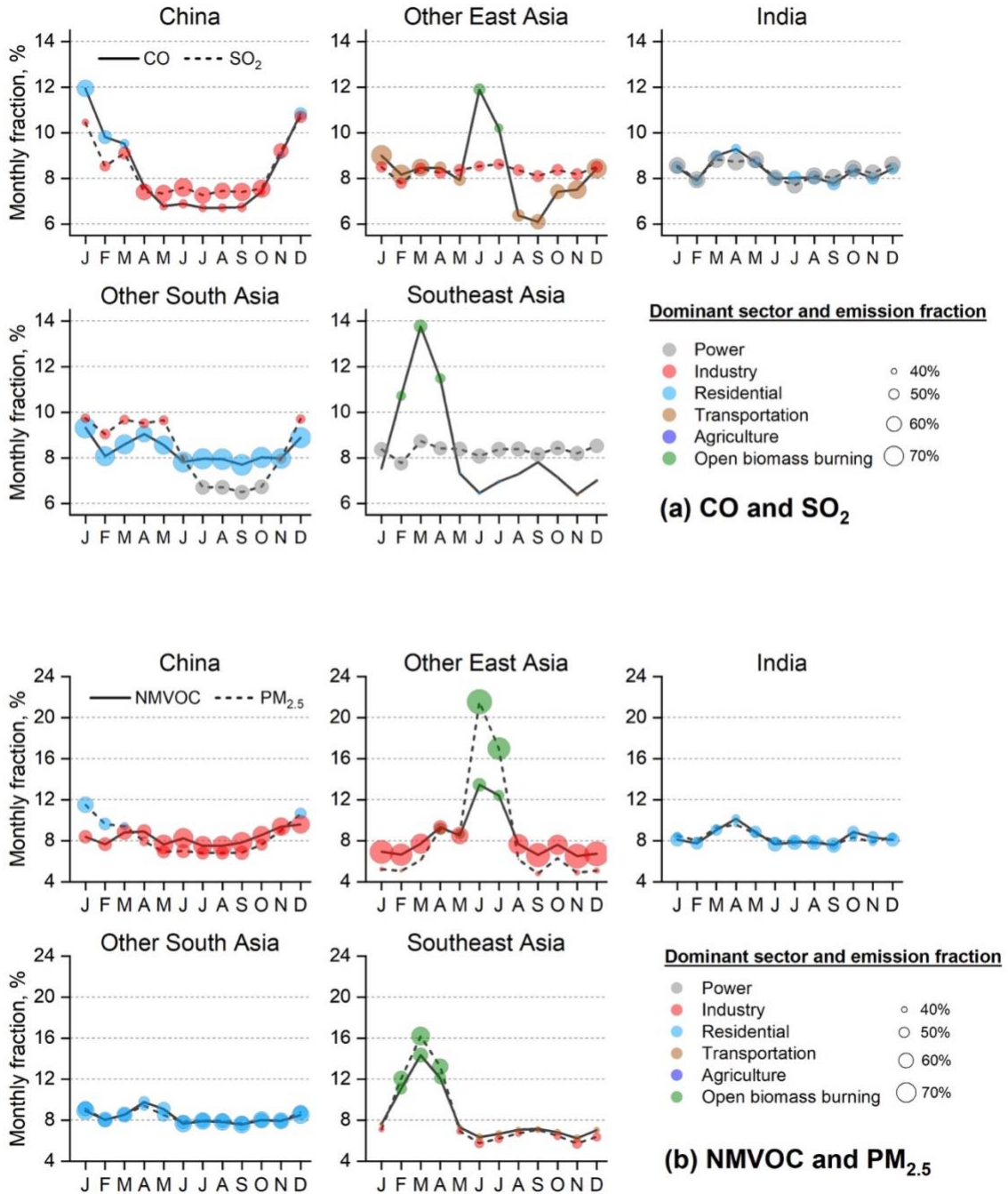
Figure 7. Monthly variations of emissions in Asian regions in 2017 for (a) CO (solid lines) and SO$_2$ (short, dashed lines), (b) NMVOC (solid lines) and PM$_{2.5}$ (short, dashed lines). For each month, the dominant sector is labeled by circle color. Circle area is scaled based on the emission fraction of the dominant sector for each month. Both anthropogenic and open biomass burning are included.

3.3 Seasonality

Monthly variations of emissions, which are highly sector dependent, are estimated in MIXv2. Within the same sector, similar monthly emission variations are found among different species as they are mainly driven by activity rates (see Fig. 6) (Li et al., 2017c). Fig. 6 and Fig. 7 illustrate the emission fractions by sectors, and the dominant sector (classified by circle color) for each month for CO, SO_2, NMVOC and $PM_{2.5}$ by regions in 2017, including both anthropogenic and open biomass burning. Contribution of the "dominant sector" is scaled to the circle area. Large circles represent the significant role of the dominant sector and small ones (near 17%) indicate the balanced contribution from six sectors. The monthly emissions patterns show large disparities varying with regions. Notable variations are estimated for emissions of China, OEA and SEA. The residential sector of China is the largest contributor in winter for CO and $PM_{2.5}$, leading to the "valley" curves. Industrial emissions show relatively high fractions in the second half of the year aiming to achieve the annual production goal, which dominate the seasonal patterns of SO_2, CO, NMVOC and $PM_{2.5}$ for most of the months. The emissions peak in summer for OEA and March for SEA are attributed to significant in-field biomass burning activities. Indian and OSA emissions show relatively small monthly variations, compared to other Asian regions. This pattern is attributed to the predominant role of the residential sector on the monthly emissions for the investigated species (as illustrated in Fig. 7). The minimal seasonal variations in surface temperature within the tropical climate of India and OSA contribute to the overall stability in monthly residential emission patterns. Thus, it's important to take both anthropogenic and open biomass sectors into account in seasonality analyses given their dominant roles varying by months, such as model evaluations based on ground/satellite/aircraft measurements.

3.4 Spatial distribution

Gridded emissions at 0.1×0.1 degree were developed in our inventory. Power plant emissions in China and India are developed on a unit basis and assigned with exact geophysical locations. For other sources, emissions are allocated to grids based on spatial proxies, such as road map, population, Gross Domestic Product (GDP), etc. The gridded MODIS fire product with high spatial resolution (up to 1km) is the essential dataset for open biomass burning emission estimation. Fig. 8 and Fig. 9 depict the spatial distribution of both CO_2 and air pollutants over Asia in 2017, showing the distinct patterns of point source, roads, and city clusters. Emission intensities of hot spots over the Indo-Gangetic Plain, spanning northern Pakistan, northern India and Bangladesh are comparable to those of northern China and Indonesia, especially for NH_3, NMVOC, BC and OC. Clear shipping routes can be seen for NO_x, SO_2, CO_2 and PM species.

Emission reductions in East Asia highlight the importance of air pollution control in Southern Asia. We show the emission changes by latitude bands from 2010 to 2017 for ozone precursors (NO_x, NMVOC, CO) and primary $PM_{2.5}$ in Fig. 10 and Fig. S2 (featuring open biomass burning). Largest reductions are estimated between 35°N ~ 40°N for NO_x (-25%), CO (-32%) and $PM_{2.5}$ (-35%) because of China's effective emission control strategies. On the other hand, NO_x

665   anthropogenic emissions have increased by 15% over 10°S ~ 0° (Southeast Asia), and +27%
666   over 10°N ~ 20°N (driven by India). Open biomass burning enlarged the emission amplitude for
667   15°S ~ 0° (Southeast Asia), while had limited effect on the trends over other latitude bands (see
668   Fig. S2). To conclude, NO_x has shifted southward in Asia. NMVOC emissions show generally
669   increasing trend over all latitude bands (+5% ~ +38%, anthropogenic). Differently, CO and
670   primary $PM_{2.5}$ show general emissions reduction since 2010 except over 15°S ~ 10°S and 10°N ~
671   20°N. These latitudinal shifts are of particular importance for the global tropospheric ozone
672   budget as ozone precursors emitted at low latitudes are more efficient at producing ozone than if
673   the same quantity of emissions is released at high latitudes (Zhang et al., 2016; Zhang et al.,
674   2021).
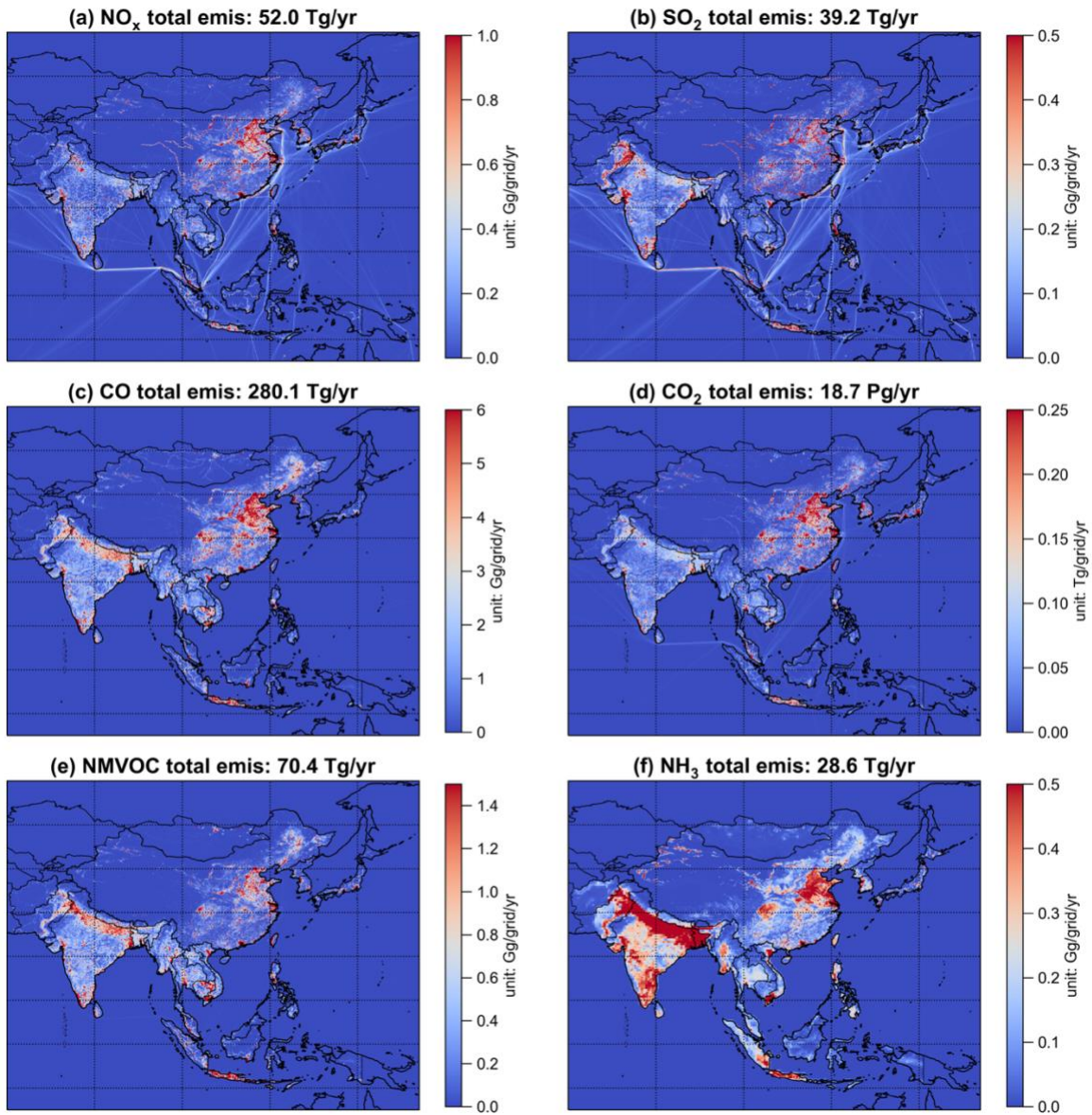
Figure 8. Spatial distribution of emissions in MIXv2 in 2017 for gaseous species.

675
676
677
678
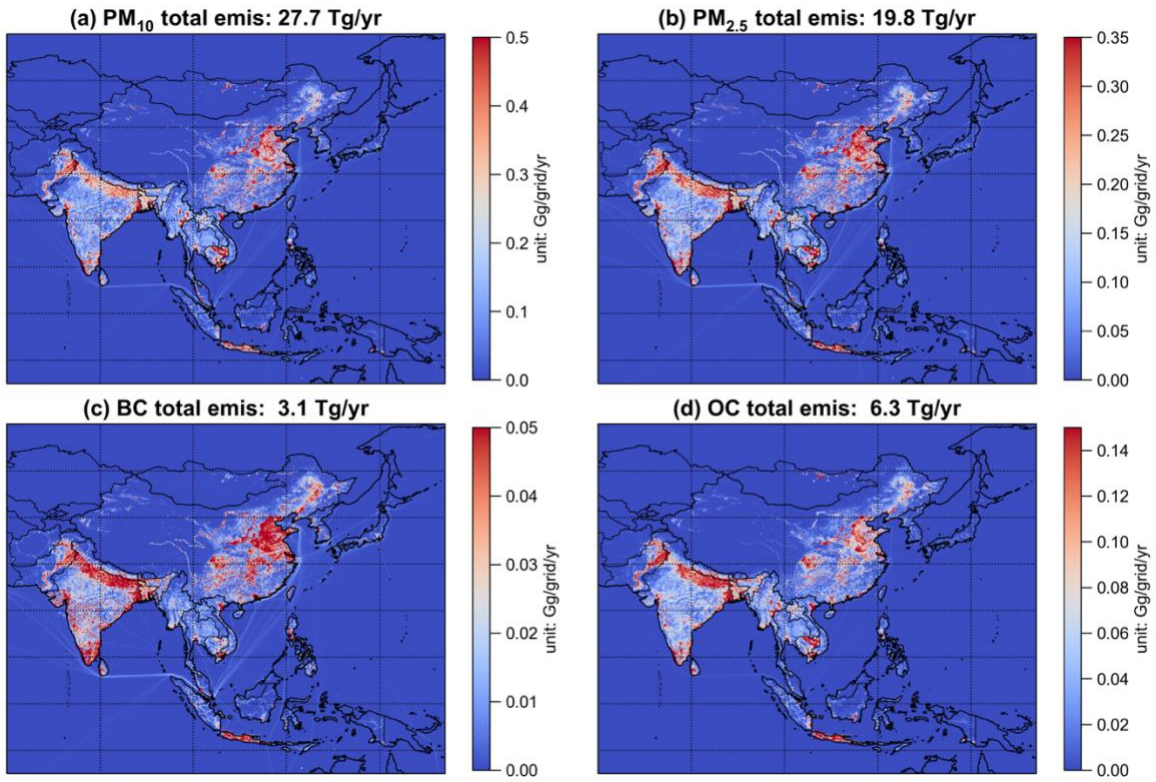
Figure 9. Spatial distribution of emissions in MIXv2 in 2017 for PM species.

682
683
(a)
684
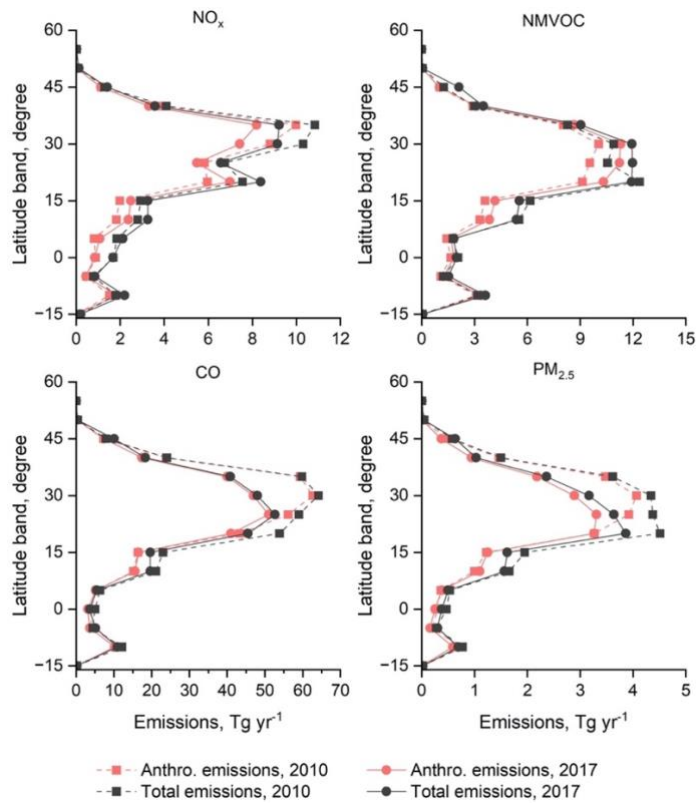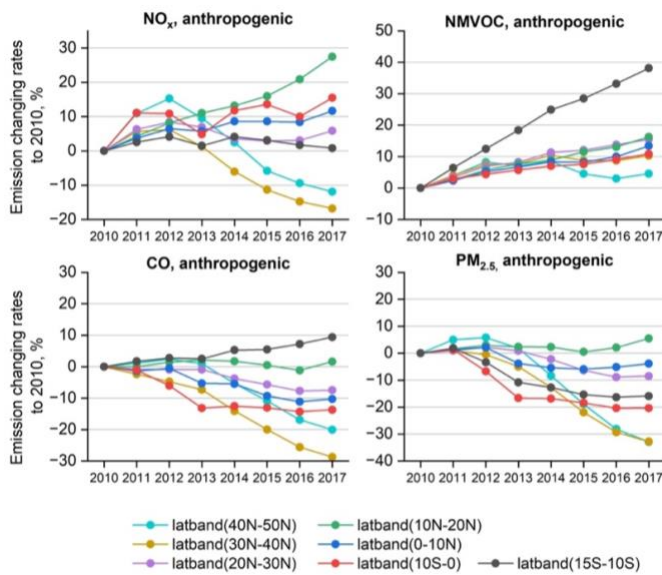
685
686
(b)
687 **Figure 10. Emissions in 2010 and 2017 (a), and anthropogenic emission changes from 2010**
688 **to 2017 (b) by latitude bands for NOₓ, NMVOC, CO and PM₂.₅. The total emissions**

33

691

3.5 Speciated NMVOC emissions

693 As one of the key precursors of ozone and secondary organic aerosols (SOA), NMVOC gain
694 more and more attention because of the emission increase due to relatively loose targeted control
695 measures. As estimated in MIXv2, Asian emissions have increased by 13% for anthropogenic
696 sources and 6% with additional open biomass burning. We speciated the total NMVOC to three
697 chemical mechanisms: SARPC99, SAPRC07 and CB05 following the profile-based approach
698 (Sect. 2.5). Emission changes during 2010-2017 by chemical groups are shown in Fig. 11.
699 Alkanes, Alkenes and Aromatics comprise 78% of the total emissions on a mole basis in 2017.
700 Driven by the growing activities in industry, emissions of Alkanes and Aromatics increased by
701 ~20% within 7 years, according to our estimates. Alkenes and Alkynes show a stable trend,
702 reflecting the combined results of emission reduction in residential and growth in industry and
703 transportation sectors. For OVOCs, especially Aldehydes, emissions decreased by 10% since
704 2010 due to reduced residential fuel combustion. Open biomass burning play a role over other
705 OVOCs (OVOCs other than Aldehydes and Ketones) emission changes. India, Southeast Asia,
706 and China are the largest contributors to the total Asian budget, with varying sector distributions
707 and driving forces by chemical groups.

708 Industry, mainly industrial solvent use, is the primary driving sector for emissions increase of
709 Alkanes (+15%) and Aromatics (+21%) in China. Moderate reductions are estimated for
710 anthropogenic OVOCs (-33% Aldehydes, +20% Ketones, -22% other OVOCs) attributed to fuel
711 transfer in the residential sector. OEA emissions show generally decreasing trends from -13%
712 (Ketones, Alkenes) to +3% (Alkynes) for anthropogenic sectors, and -10% (Ketones, Aromatics,
713 Others) to +25% (Other OVOCs) with additional open biomass burning. Industrial emissions
714 have decreased over all chemical groups for OEA. Similar sectoral distributions across chemical
715 species are found for India and OSA, dominated by the residential and transportation sectors.
716 More than 29% emissions growth are estimated for Alkanes and Aromatics, driven by industry,
717 residential, and transportation sectors in India and OSA. In SEA, ～20% increases are estimated
718 for emissions of Alkanes and Aromatics, and minor changes for Alkenes, Alkynes, Aldehydes
719 and Ketones (within 10%) during 2010-2017. OVOCs emissions in 2017 are 25% lower than the
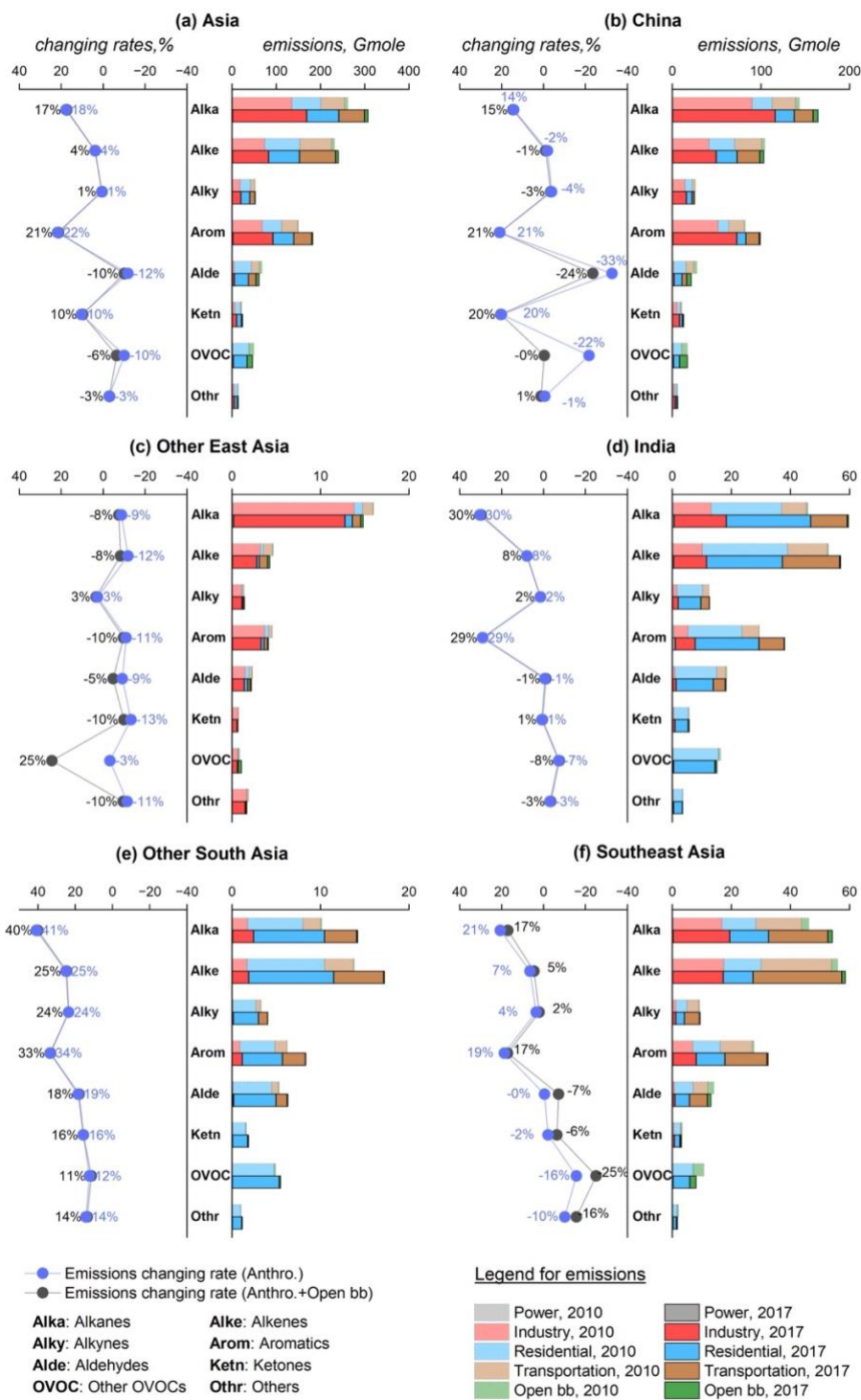720 values in 2010, contributed by residential sources and open biomass burning.

721

722

723

724

725

Figure 11. Emissions in 2010 and 2017 (right columns) and the emission changing rates from 2010–2017 (left columns) of NMVOCs by chemical groups. For each country/region,

35

729 the left column represents the emission changing rates (in unit of %), and the right column
730 shows the emissions by sectors in 2010 and 2017. Chemical groups are lumped from the
731 SAPRC07 species following Table S4. Open bb denotes open biomass burning.
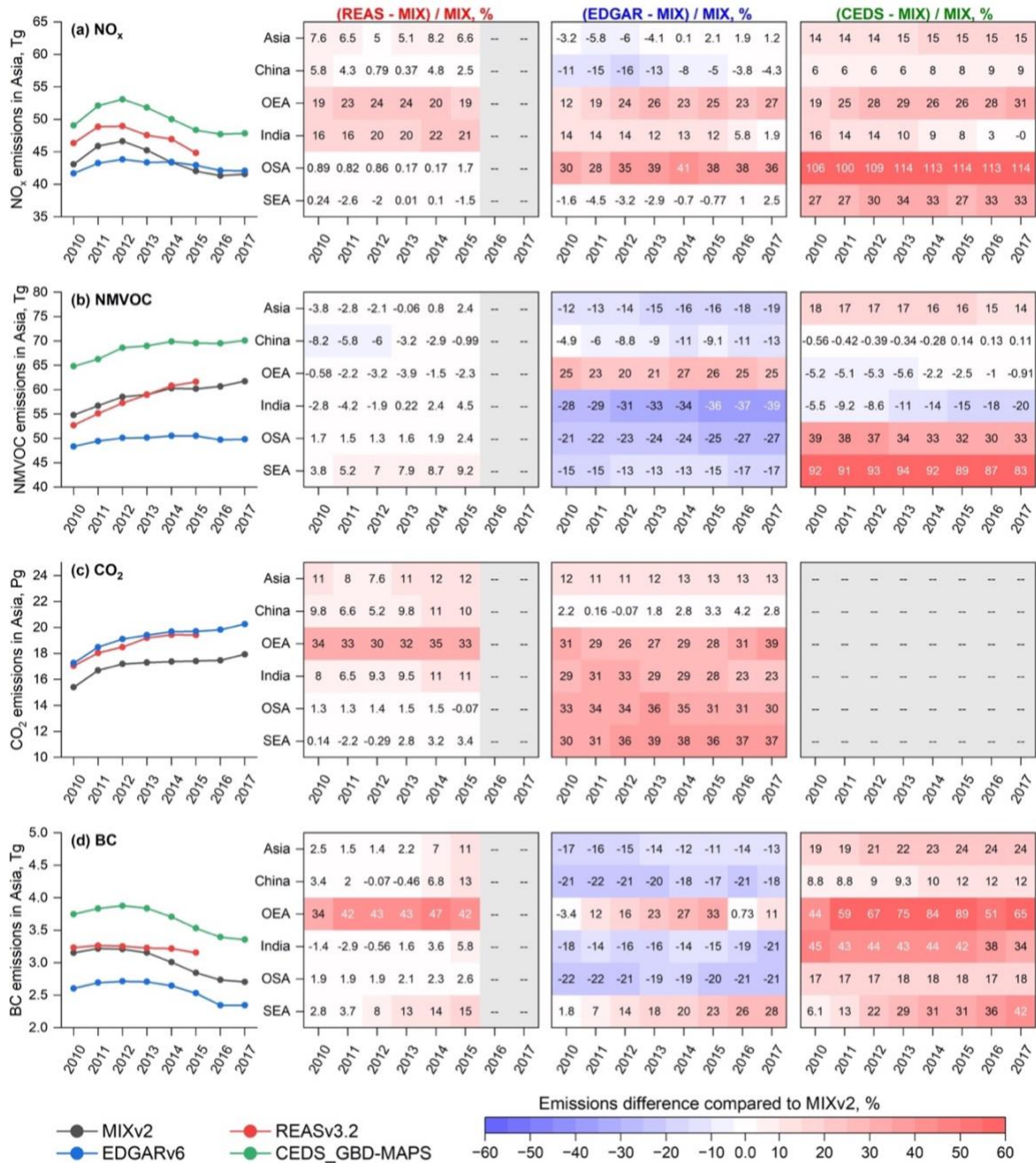
Figure 12. Emission comparisons for anthropogenic sources between MIXv2, REASv3.2, EDGARv6, and CEDS_GBD-MAPs for (a) NO$_x$, (b) NMVOC, (c) CO$_2$ and (d) BC during 2010–2017 by Asian regions.

4. Inter-comparisons with other bottom-up and top-down emission estimates

Table 5. Top-down emission trends since 2010 over Asia.

Species	Estimates	Region	Period	AGR (% yr^{-1}) [a]	Techniques
NO$_x$	Krotkov et al. (2016)	E China	2010-2015	-4.9	Satellite
	Liu et al. (2016)	E China	2010-2015	-5.1	Satellite
	Miyazaki et al. (2017)	China	2010-2016	-2.6	Inverse Modeling
	van der A et al. (2017)	E China	2010-2015	-1.7	Inverse Modeling
	Georgoulias et al. (2019)	China	2011-2018	-6.2	Satellite
	Hou et al. (2019)	China	2010-2017	-4.1	Satellite
	Itahashi et al. (2019)	China	2010-2016	-1.6	Inverse Modeling
	Zhang et al. (2019)	China	2010-2017	-5.0	Satellite
	MIXv2	China	2010-2017	-2.6	Bottom-up
	Krotkov et al. (2016)	India	2010-2015	3.4	Satellite
	Miyazaki et al. (2017)	India	2010-2016	2.5	Inverse Modeling
	Itahashi et al. (2019)	India	2010-2016	6.0	Inverse Modeling
	MIXv2	India	2010-2017	4.7	Bottom-up
SO$_2$	Tropospheric Chemistry Reanalysis (TCR-2) [b]	China	2010-2017	-7.1	Inverse Modeling
	Krotkov et al. (2016)	E China	2010-2015	-11.0	Satellite
	van der A et al. (2017)	E China	2010-2015	-8.0	Inverse Modeling
	C. Li et al. (2017)	China	2010-2016	-18.0	Inverse Modeling
	Koukouli et al. (2018)	China	2010-2015	-6.2	Inverse Modeling
	Zhang et al. (2019)	China	2010-2017	-4.0	Satellite
	Qu et al. (2019) [c]	China	2010-2017	-4.0	Inverse Modeling
	MIXv2	China	2010-2017	-12.9	Bottom-up
	TCR-2 [b]	India	2010-2017	1.2	Inverse Modeling
	Krotkov et al. (2016)	India	2010-2015	6.0	Satellite
	C. Li et al. (2017)	India	2010-2016	3.4	Inverse Modeling
	Qu et al. (2019) [c]	India	2010-2017	1.7	Inverse Modeling
	MIXv2	India	2010-2017	5.6	Bottom-up
CO	Jiang et al. (2017) [d]	China	2010-2015	-2.8	Inverse Modeling
	Zheng et al. (2019) [e]	China	2010-2017	-2.1	Inverse Modeling
	MIX v2	China	2010-2017	-4.4	Bottom-up
	Jiang et al. (2017) [d]	India / SEA	2010-2015	2.9	Inverse Modeling

	Zheng et al. (2019)	India	2010-2017	-1.7	Inverse Modeling
	MIXv2	India	2010-2017	0.4	Bottom-up
	Zheng et al. (2019)	SEA (an) [f]	2010-2017	-2.4	Inverse Modeling
	MIXv2	SEA (an)	2010-2017	-0.8	Bottom-up
	Jiang et al. (2017)	SEA (bb) [g]	2010-2014 [2010-2015] [h]	6.3 [51.6] [h]	Inverse Modeling
	Zheng et al. (2019)	SEA (bb)	2010-2017 [2010-2015]	-11.2 [40.1]	Inverse Modeling
	MIXv2	SEA (bb)	2010-2017 [2010-2015]	-7.9 [40.1]	Bottom-up
NMVOC	Stavrakou et al. (2017)	China	2010-2014	1.7	Inverse Modeling [i]
	Zhang et al. (2019)	China	2010-2017	1.0	Satellite [i]
	MIXv2	China	2010-2017	1.3	Bottom-up
NH_3	Warner et al. (2017)	China	2010-2016	2.2	Satellite
	Damme et al. (2021)	China	2010-2017	5.5	Satellite
	MIXv2	China	2010-2017	-1.2	Bottom-up
	Damme et al. (2021)	India	2010-2017	0.5	Satellite
	MIXv2	India	2010-2017	2.2	Bottom-up
	Damme et al. (2021)	SEA	2010-2017 [2010-2015]	-2.7 [8.9]	Satellite
	MIXv2	SEA	2010-2017 [2010-2015]	1.7 [5.3]	Bottom-up

740
741 [a] AGR: Annual Growth Rate.
742 [b] Elguindi et al. (2020)
743 [c] Top-down estimates based on NASA products
744 [d] estimates derived from MOPITT profiles
745 [e] the results of full inversion # 3 are summarized here
746 [f] Southeast Asia for anthropogenic sources
747 [g] Southeast Asia for open biomass burning
748 [h] the growth rates between 2010 and 2015 are listed in square brackets because 2015 is a El Niño year
749 [i] HCHO columns are used

750

751 To provide a potential uncertainty range of MIXv2, we compared our estimates with both
752 regional and global inventories, as well as top-down estimates from previous satellite-based and
753 inverse modeling studies. Figure 12 shows the emission comparisons of MIXv2 with REASv3.2,
754 EDGARv6, and CEDS_GBD-MAPS (referred to as CEDS) (McDuffie et al., 2020) by Asian
755 regions during 2010-2017 for NO_x, NMVOC, CO_2 and BC. REAS and MIX show the best
756 agreement (differing within 12%) as expected because REAS was used as default estimates over
757 Asia. Similar trends are found between REAS and MIX for all species except BC. The trends of
758 NO_x in EDGAR are different than the others which peak in 2012, indicating the needs of re-
759 visiting the parameterization of control policies in East Asia in the global inventory system.

760   EDGAR estimates are within 20% difference with MIXv2 for the whole Asia, but with higher
761   discrepancies over OEA, OSA and SEA. NMVOCs are 12%~19% lower in EDGAR, mainly for
762   India and OSA. Notably, the emission discrepancies have grown larger in recent years, attributed
763   to the differences in emissions trends. EDGAR's NMVOC emissions show a relatively flat trend,
764   in contrast to the continuously increasing pattern of MIX. Emissions of CO_2 over OEA, OSA and
765   SEA seem to be uncertain, with more than 30% difference between EDGAR and MIX. Similarly,
766   the emission differences of BC in SEA need to be considered when used in climate model
767   simulations. The emission trends of CEDS are consistent with those of MIX because MEIC was
768   applied to scale the emissions in the CEDS system (McDuffie et al., 2020). However, compared
769   to MIX, CEDS emissions are generally higher across regions and species, with large
770   discrepancies over OEA (+65% for BC, +31% for NO_x in 2017), India (+34% for BC), OSA
771   (+114% for NO_x, +33% for NMVOCs) and SEA (+33% for NO_x, +83% for NMVOCs, +42% for
772   BC). These comparisons highlight the potential uncertainties of bottom-up emission inventories
773   over South Asia and Southeast Asia where information is still limited compared to East Asia.
774   More validations and revisions are needed to identify the reasons of the discrepancies and narrow
775   down the gaps.

776   Table 5 summarizes the top-down emission annual growth rates since 2010 as derived from
777   satellite retrievals and inverse modeling studies. MIX trends show high consistency with the top-
778   down estimates, especially the inverse modeling results. Decreasing trends since the peak in
779   2012 for NO_x emissions in China are validated from space (Georgoulias et al., 2019; Hou et al.,
780   2019; Itahashi et al., 2019; Krotkov et al., 2016; Liu et al., 2016; Miyazaki et al., 2017; van der
781   A et al., 2017; Zhang et al., 2019). The annual growth rates derived directly from satellite
782   retrievals (-4.1 ~ -6.2 % yr^{-1}) are in general larger than those from inverse modeling (-1.6 ~ -
783   2.6 % yr^{-1}) which jointly account for the air transport and chemical non-linearity. Similar
784   declining trends are found from top-down estimates of SO_2 (Elguindi et al., 2020; Koukouli et
785   al., 2018; Krotkov et al., 2016; Li et al., 2017a; Qu et al., 2019; van der A et al., 2017; Zhang et
786   al., 2019) and CO (Jiang et al., 2017; Zheng et al., 2019) over China. For India, emissions have
787   been detected to grow continuously from space for NO_x and SO_2, with growth rates consistent
788   with the inventory estimation. Slightly increasing trend is detected from space for HCHO in
789   China, as an indicator of NMVOC emissions (Stavrakou et al., 2017; Zhang et al., 2019). 2015 is
790   an El Niño year, and this climate anomaly turns out to significantly affect the emissions trends of
791   CO and NH_3 in SEA (Van Damme et al., 2021). More inverse modeling work by combining
792   multiple species are needed for NH_3 over Asia to shed light on the uncertainty range of inventory
793   estimation.

794

795

796

797

798

5. Concluding remarks

In this work, we developed the MIXv2 emission inventory for Asia during 2010-2017 resolved with relatively high spatial resolution (0.1°) and temporal resolution (monthly), and detailed chemical speciation (SAPRC99, SAPRC07, CB05). MEICv2, PKU-NH$_3$, PKU-Biomass, ANL-India, CAPSS, JPN are used to represent the best available emission inventories for China, India, the Republic of Korea, and Japan, fill-gaped with REASv3 and GFEDv4. Constructing a long-term mosaic emission inventory requires substantial international collaborations. MIXv2 was developed based on the state-of-the-art updated emission inputs under the framework of MICS-Asia Phase IV, and is now ready to feed the atmospheric chemistry models and improve chemistry-climate models for long-term analyses. With high spatial resolution up to 0.1°, MIXv2 is capable of supporting model activities at regional and even local scales. As far as we know, MIXv2 is the first mosaic inventory with both anthropogenic and open biomass burning estimated by incorporating local emission inventories. Emissions are aggregated to seven sectors in MIX: power, industry, residential, transportation, agriculture as anthropogenic sources, along with open biomass burning and shipping. With three chemical mechanisms developed using a consistent speciation framework, MIXv2 can be used in most of the atmospheric models even for those configured with updates on ozone and secondary organic aerosols formation. MIXv2 also has CO_2 emissions based on the same emissions model for 9 air pollutants (NO_x, SO_2, CO, NMVOC, NH_3, PM_{10}, $PM_{2.5}$, BC, OC), providing a consistent dataset for climate-air quality nexus research. Gridded monthly emissions are publicly available at https://csl.noaa.gov/groups/csl4/modeldata/data/Li2023/.

Driving forces of the emission changes during 2010-2017 are investigated based on MIXv2. Significant emission reductions from anthropogenic sources are found for SO_2, CO, PM_{10}, $PM_{2.5}$, BC, and OC, driven by effective clean air actions conducted over China and Other East Asia. India, Other South Asia, and Southeast Asia show continuously increasing emissions trends since 2010, limiting the emissions reduction for Asia as a whole. On the contrary, NMVOC and NH_3 emissions increased or remained flat due to insufficient targeted control measures. Open biomass burning is the largest contributor to Southeast Asia for emissions of CO, NMVOC and OC. NO_x emissions have shown clear latitudinal shifts southward in Asia, which is important for global tropospheric ozone budget. Our estimated trends are in general consistent with those derived from satellite retrievals, especially results from inverse modeling.

Further validation is needed for MIXv2 for better understanding of the data reliability. Inverse modeling studies on NMVOC and NH_3 are still limited, partly attributed to the lack of available measurement data over Asia. With the launch of the Geostationary Environment Monitoring Spectrometer (GEMS) and the availability of hourly retrievals of atmospheric composition, top-down constraints on both emissions spatial distributions and temporal variations are now possible (Kim et al., 2020) on the scale of Asia. In-situ measurements, aircraft and satellite data should be combined with inventory and model simulations to improve emission estimates in the future.

839

6. Data availability

MIXv2 gridded monthly emissions data for both anthropogenic and open biomass burning for
2010-2017 by 10 species and 7 sectors are available at:
https://csl.noaa.gov/groups/csl4/modeldata/data/Li2023/, and also shared in
http://meicmodel.org/dataset-mixv2. Emission estimates by Asian countries and sectors are
summarized in the supplement. Daily open biomass burning emissions are available upon
request.

847

7. Author contribution

M. Li, Q. Zhang, J. Kurokawa and J. Woo initiated the research topic. M. Li developed the
emissions model, conducted the analyses, and prepared the paper. J. Kurokawa, Q. Zhang, J.
Woo, T. Morikawa, S. Chatani, Z. Lu, Y. Song, G. Geng, H. Hu, J. Kim provided the regional
emissions data. O. R. Cooper and B. C. McDonald have contributed by providing the computing
resources and data analyses. All co-authors have contributed with paper revision comments.

854

8. Competing interests

At least one of our co-authors are members of the editorial board of ACP. The peer-review
process was guided by an independent editor, and the authors have also no other competing
interests to declare.

859

9. Acknowledgement

861

883

884

885

References

Adam, M. G., Tran, P. T. M., Bolan, N., and Balasubramanian, R.: Biomass burning-derived airborne particulate matter in Southeast Asia: A critical review, Journal of Hazardous Materials, 407, 124760, 2021.

Akagi, S. K., Yokelson, R. J., Wiedinmyer, C., Alvarado, M. J., Reid, J. S., Karl, T., Crounse, J. D., and Wennberg, P. O.: Emission factors for open and domestic biomass burning for use in atmospheric models, Atmos. Chem. Phys., 11, 4039-4072, 2011.

Andreae, M. O. and Merlet, P.: Emission of trace gases and aerosols from biomass burning, Global Biogeochemical Cycles, 15, 955-966, 2001.

Anwar, M. N., Shabbir, M., Tahir, E., Iftikhar, M., Saif, H., Tahir, A., Murtaza, M. A., Khokhar, M. F., Rehan, M., Aghbashlo, M., Tabatabaei, M., and Nizami, A.-S.: Emerging challenges of air pollution and particulate matter in China, India, and Pakistan and mitigating solutions, Journal of Hazardous Materials, 416, 125851, 2021.

Carter, W. P. L.: Development of a database for chemical mechanism assignments for volatile organic emissions, Journal of the Air & Waste Management Association, 65, 1171-1184, 2015.

Chatani, S., Shimadera, H., Itahashi, S., and Yamaji, K.: Comprehensive analyses of source sensitivities and apportionments of PM2.5 and ozone over Japan via multiple numerical techniques, Atmos. Chem. Phys., 20, 10311-10329, 2020.

Chatani, S., Yamaji, K., Sakurai, T., Itahashi, S., Shimadera, H., Kitayama, K., and Hayami, H.: Overview of Model Inter-Comparison in Japan's Study for Reference Air Quality Modeling (J-STREAM), Atmosphere, 9, 19, 2018.

Chen, L., Gao, Y., Zhang, M., Fu, J. S., Zhu, J., Liao, H., Li, J., Huang, K., Ge, B., Wang, X., Lam, Y. F., Lin, C. Y., Itahashi, S., Nagashima, T., Kajino, M., Yamaji, K., Wang, Z., and Kurokawa, J.: MICS-Asia III: multi-model comparison and evaluation of aerosol over East Asia, Atmos. Chem. Phys., 19, 11911-11937, 2019.

Crippa, M., Guizzardi, D., Butler, T., Keating, T., Wu, R., Kaminski, J., Kuenen, J., Kurokawa, J., Chatani, S., Morikawa, T., Pouliot, G., Racine, J., Moran, M. D., Klimont, Z., Manseau, P. M., Mashayekhi, R., Henderson, B. H., Smith, S. J., Suchyta, H., Muntean, M., Solazzo, E., Banja, M., Schaaf, E., Pagani, F., Woo, J. H., Kim, J., Monforti-Ferrario, F., Pisoni, E., Zhang, J., Niemi, D., Sassi, M., Ansari, T., and Foley, K.: The HTAP_v3 emission mosaic: merging regional and global monthly emissions (2000–2018) to support air quality modelling and policies, Earth Syst. Sci. Data, 15, 2667-2694, 2023.

Crippa, M., Guizzardi, D., Muntean, M., Schaaf, E., Dentener, F., van Aardenne, J. A., Monni, S., Doering, U., Olivier, J. G. J., Pagliari, V., and Janssens-Maenhout, G.: Gridded emissions of air pollutants for the period 1970–2012 within EDGAR v4.3.2, Earth Syst. Sci. Data, 10, 1987-2013, 2018.

923 Elguindi, N., Granier, C., Stavrakou, T., Darras, S., Bauwens, M., Cao, H., Chen, C., Denier van
924 der Gon, H. A. C., Dubovik, O., Fu, T. M., Henze, D. K., Jiang, Z., Keita, S., Kuenen, J. J. P.,
925 Kurokawa, J., Liousse, C., Miyazaki, K., Müller, J. F., Qu, Z., Solmon, F., and Zheng, B.:
926 Intercomparison of Magnitudes and Trends in Anthropogenic Surface Emissions From Bottom-
927 Up Inventories, Top-Down Estimates, and Emission Scenarios, Earth's Future, 8,
928 e2020EF001520, 2020.

929 Feng, Z., Xu, Y., Kobayashi, K., Dai, L., Zhang, T., Agathokleous, E., Calatayud, V., Paoletti,
930 E., Mukherjee, A., Agrawal, M., Park, R. J., Oak, Y. J., and Yue, X.: Ozone pollution threatens
931 the production of major staple crops in East Asia, Nature Food, 3, 47-56, 2022.

932 Field, R. D., van der Werf, G. R., Fanin, T., Fetzer, E. J., Fuller, R., Jethva, H., Levy, R.,
933 Livesey, N. J., Luo, M., Torres, O., and Worden, H. M.: Indonesian fire activity and smoke
934 pollution in 2015 show persistent nonlinear sensitivity to El Niño-induced drought, Proceedings
935 of the National Academy of Sciences, 113, 9204-9209, 2016.

936 Fiore, A. M., Naik, V., and Leibensperger, E. M.: Air Quality and Climate Connections, Journal
937 of the Air & Waste Management Association, 65, 645-685, 2015.

938 Gao, M., Han, Z., Liu, Z., Li, M., Xin, J., Tao, Z., Li, J., Kang, J. E., Huang, K., Dong, X.,
939 Zhuang, B., Li, S., Ge, B., Wu, Q., Cheng, Y., Wang, Y., Lee, H. J., Kim, C. H., Fu, J. S., Wang,
940 T., Chin, M., Woo, J. H., Zhang, Q., Wang, Z., and Carmichael, G. R.: Air quality and climate
941 change, Topic 3 of the Model Inter-Comparison Study for Asia Phase III (MICS-Asia III) –
942 Part 1: Overview and model evaluation, Atmos. Chem. Phys., 18, 4859-4884, 2018.

943 Geng, G., Zheng, Y., Zhang, Q., Xue, T., Zhao, H., Tong, D., Zheng, B., Li, M., Liu, F., Hong,
944 C., He, K., and Davis, S. J.: Drivers of PM2.5 air pollution deaths in China 2002–2017, Nature
945 Geoscience, 14, 645-650, 2021.

946 Georgoulias, A. K., van der A, R. J., Stammes, P., Boersma, K. F., and Eskes, H. J.: Trends and
947 trend reversal detection in 2 decades of tropospheric NO2 satellite observations, Atmos. Chem.
948 Phys., 19, 6269-6294, 2019.

949 Hammer, M. S., van Donkelaar, A., Li, C., Lyapustin, A., Sayer, A. M., Hsu, N. C., Levy, R. C.,
950 Garay, M. J., Kalashnikova, O. V., Kahn, R. A., Brauer, M., Apte, J. S., Henze, D. K., Zhang, L.,
951 Zhang, Q., Ford, B., Pierce, J. R., and Martin, R. V.: Global Estimates and Long-Term Trends of
952 Fine Particulate Matter Concentrations (1998–2018), Environmental Science & Technology, 54,
953 7879-7890, 2020.

954 Hou, Y., Wang, L., Zhou, Y., Wang, S., Liu, W., and Zhu, J.: Analysis of the tropospheric
955 column nitrogen dioxide over China based on satellite observations during 2008–2017,
956 Atmospheric Pollution Research, 10, 651-655, 2019.

957 Huang, X., Li, M., Li, J., and Song, Y.: A high-resolution emission inventory of crop burning in
958 fields in China based on MODIS Thermal Anomalies/Fire products, Atmospheric Environment,
959 50, 9-15, 2012a.

960 Huang, X., Song, Y., Li, M., Li, J., Huo, Q., Cai, X., Zhu, T., Hu, M., and Zhang, H.: A high-
961 resolution ammonia emission inventory in China, Global Biogeochemical Cycles, 26, 2012b.

962 Itahashi, S., Ge, B., Sato, K., Fu, J. S., Wang, X., Yamaji, K., Nagashima, T., Li, J., Kajino, M.,
963 Liao, H., Zhang, M., Wang, Z., Li, M., Kurokawa, J., Carmichael, G. R., and Wang, Z.: MICS-
964 Asia III: overview of model intercomparison and evaluation of acid deposition over Asia, Atmos.
965 Chem. Phys., 20, 2667-2693, 2020.

966 Itahashi, S., Yumimoto, K., Kurokawa, J.-i., Morino, Y., Nagashima, T., Miyazaki, K., Maki, T.,
967 and Ohara, T.: Inverse estimation of NOx emissions over China and India 2005–2016:
968 contrasting recent trends and future perspectives, Environmental Research Letters, 14, 124020,
969 2019.

970 Jacob, D. J. and Winner, D. A.: Effect of climate change on air quality, Atmospheric
971 Environment, 43, 51-63, 2009.

972 Janssens-Maenhout, G., Crippa, M., Guizzardi, D., Dentener, F., Muntean, M., Pouliot, G.,
973 Keating, T., Zhang, Q., Kurokawa, J., Wankmüller, R., Denier van der Gon, H., Kuenen, J. J. P.,
974 Klimont, Z., Frost, G., Darras, S., Koffi, B., and Li, M.: HTAP_v2.2: a mosaic of regional and
975 global emission grid maps for 2008 and 2010 to study hemispheric transport of air pollution,
976 Atmos. Chem. Phys., 15, 11411-11432, 2015.

977 Janssens-Maenhout, G., Crippa, M., Guizzardi, D., Muntean, M., Schaaf, E., Dentener, F.,
978 Bergamaschi, P., Pagliari, V., Olivier, J. G. J., Peters, J. A. H. W., van Aardenne, J. A., Monni,
979 S., Doering, U., Petrescu, A. M. R., Solazzo, E., and Oreggioni, G. D.: EDGAR v4.3.2 Global
980 Atlas of the three major greenhouse gas emissions for the period 1970–2012, Earth Syst. Sci.
981 Data, 11, 959-1002, 2019.

982 Jiang, Z., Worden, J. R., Worden, H., Deeter, M., Jones, D. B. A., Arellano, A. F., and Henze, D.
983 K.: A 15-year record of CO emissions constrained by MOPITT CO observations, Atmos. Chem.
984 Phys., 17, 4565-4583, 2017.

985 Kang, Y., Liu, M., Song, Y., Huang, X., Yao, H., Cai, X., Zhang, H., Kang, L., Liu, X., Yan, X.,
986 He, H., Zhang, Q., Shao, M., and Zhu, T.: High-resolution ammonia emissions inventories in
987 China from 1980 to 2012, Atmos. Chem. Phys., 16, 2043-2058, 2016.

988 Kim, J., Jeong, U., Ahn, M.-H., Kim, J. H., Park, R. J., Lee, H., Song, C. H., Choi, Y.-S., Lee,
989 K.-H., Yoo, J.-M., Jeong, M.-J., Park, S. K., Lee, K.-M., Song, C.-K., Kim, S.-W., Kim, Y. J.,
990 Kim, S.-W., Kim, M., Go, S., Liu, X., Chance, K., Chan Miller, C., Al-Saadi, J., Veihelmann, B.,
991 Bhartia, P. K., Torres, O., Abad, G. G., Haffner, D. P., Ko, D. H., Lee, S. H., Woo, J.-H., Chong,
992 H., Park, S. S., Nicks, D., Choi, W. J., Moon, K.-J., Cho, A., Yoon, J., Kim, S.-k., Hong, H., Lee,
993 K., Lee, H., Lee, S., Choi, M., Veefkind, P., Levelt, P. F., Edwards, D. P., Kang, M., Eo, M.,
994 Bak, J., Baek, K., Kwon, H.-A., Yang, J., Park, J., Han, K. M., Kim, B.-R., Shin, H.-W., Choi,
995 H., Lee, E., Chong, J., Cha, Y., Koo, J.-H., Irie, H., Hayashida, S., Kasai, Y., Kanaya, Y., Liu,
996 C., Lin, J., Crawford, J. H., Carmichael, G. R., Newchurch, M. J., Lefer, B. L., Herman, J. R.,
997 Swap, R. J., Lau, A. K. H., Kurosu, T. P., Jaross, G., Ahlers, B., Dobber, M., McElroy, C. T.,
998 and Choi, Y.: New Era of Air Quality Monitoring from Space: Geostationary Environment
999 Monitoring Spectrometer (GEMS), Bulletin of the American Meteorological Society, 101, E1-
1000 E22, 2020.

1001 Klausbruckner, C., Annegarn, H., Henneman, L. R. F., and Rafaj, P.: A policy review of
1002 synergies and trade-offs in South African climate change mitigation and air pollution control
1003 strategies, Environmental Science & Policy, 57, 70-78, 2016.

1004 Koukouli, M. E., Theys, N., Ding, J., Zyrichidou, I., Mijling, B., Balis, D., and van der A, R. J.:
1005 Updated SO2 emission estimates over China using OMI/Aura observations, Atmos. Meas. Tech.,
1006 11, 1817-1832, 2018.

1007 Krotkov, N. A., McLinden, C. A., Li, C., Lamsal, L. N., Celarier, E. A., Marchenko, S. V.,
1008 Swartz, W. H., Bucsela, E. J., Joiner, J., Duncan, B. N., Boersma, K. F., Veefkind, J. P., Levelt,
1009 P. F., Fioletov, V. E., Dickerson, R. R., He, H., Lu, Z., and Streets, D. G.: Aura OMI
1010 observations of regional SO2 and NO2 pollution changes from 2005 to 2015, Atmos. Chem.
1011 Phys., 16, 4605-4629, 2016.

1012 Kurokawa, J. and Ohara, T.: Long-term historical trends in air pollutant emissions in Asia:
1013 Regional Emission inventory in ASia (REAS) version 3, Atmos. Chem. Phys., 20, 12761-12793,
1014 2020.

1015 Lee, D.-G., Lee, Y.-M., Jang, K.-W., Yoo, C., Kang, K.-H., Lee, J.-H., Jung, S.-W., Park, J.-M.,
1016 Lee, S.-B., Han, J.-S., Hong, J.-H., and Lee, S.-J.: Korean National Emissions Inventory System
1017 and 2007 Air Pollutant Emissions, Asian Journal of Atmospheric Environment, 5, 278-291,
1018 2011.

1019 Lei, Y., Zhang, Q., He, K. B., and Streets, D. G.: Primary anthropogenic aerosol emission trends
1020 for China, 1990–2005, Atmos. Chem. Phys., 11, 931-954, 2011.

1021 Li, C., McLinden, C., Fioletov, V., Krotkov, N., Carn, S., Joiner, J., Streets, D., He, H., Ren, X.,
1022 Li, Z., and Dickerson, R. R.: India Is Overtaking China as the World's Largest Emitter of
1023 Anthropogenic Sulfur Dioxide, Scientific Reports, 7, 14304, 2017a.

1024 Li, K., Jacob, D. J., Liao, H., Zhu, J., Shah, V., Shen, L., Bates, K. H., Zhang, Q., and Zhai, S.: A
1025 two-pollutant strategy for improving ozone and particulate air quality in China, Nature
1026 Geoscience, 12, 906-910, 2019a.

1027 Li, M., Klimont, Z., Zhang, Q., Martin, R. V., Zheng, B., Heyes, C., Cofala, J., Zhang, Y., and
1028 He, K.: Comparison and evaluation of anthropogenic emissions of SO2 and NOx over China,
1029 Atmos. Chem. Phys., 18, 3433-3456, 2018.

1030 Li, M., Liu, H., Geng, G., Hong, C., Liu, F., Song, Y., Tong, D., Zheng, B., Cui, H., Man, H.,
1031 Zhang, Q., and He, K.: Anthropogenic emission inventories in China: a review, National Science
1032 Review, 4, 834-866, 2017b.

1033 Li, M., Zhang, Q., Kurokawa, J. I., Woo, J. H., He, K., Lu, Z., Ohara, T., Song, Y., Streets, D.
1034 G., Carmichael, G. R., Cheng, Y., Hong, C., Huo, H., Jiang, X., Kang, S., Liu, F., Su, H., and
1035 Zheng, B.: MIX: a mosaic Asian anthropogenic emission inventory under the international
1036 collaboration framework of the MICS-Asia and HTAP, Atmos. Chem. Phys., 17, 935-963,
1037 2017c.

Li, M., Zhang, Q., Streets, D. G., He, K. B., Cheng, Y. F., Emmons, L. K., Huo, H., Kang, S. C., Lu, Z., Shao, M., Su, H., Yu, X., and Zhang, Y.: Mapping Asian anthropogenic emissions of non-methane volatile organic compounds to multiple chemical mechanisms, Atmos. Chem. Phys., 14, 5617-5638, 2014.

Li, M., Zhang, Q., Zheng, B., Tong, D., Lei, Y., Liu, F., Hong, C., Kang, S., Yan, L., Zhang, Y., Bo, Y., Su, H., Cheng, Y., and He, K.: Persistent growth of anthropogenic non-methane volatile organic compound (NMVOC) emissions in China during 1990–2017: drivers, speciation and ozone formation potential, Atmos. Chem. Phys., 19, 8897-8913, 2019b.

Liu, F., Zhang, Q., Tong, D., Zheng, B., Li, M., Huo, H., and He, K. B.: High-resolution inventory of technologies, activities, and emissions of coal-fired power plants in China from 1990 to 2010, Atmos. Chem. Phys., 15, 13299-13317, 2015.

Liu, F., Zhang, Q., van der A, R. J., Zheng, B., Tong, D., Yan, L., Zheng, Y., and He, K.: Recent reduction in NOx emissions over China: synthesis of satellite observations and emission inventories, Environmental Research Letters, 11, 114002, 2016.

Lu, Z. and Streets, D. G.: Increase in NOx Emissions from Indian Thermal Power Plants during 1996–2010: Unit-Based Inventories and Multisatellite Observations, Environmental Science & Technology, 46, 7463-7470, 2012.

Lu, Z., Zhang, Q., and Streets, D. G.: Sulfur dioxide and primary carbonaceous aerosol emissions in China and India, 1996–2010, Atmos. Chem. Phys., 11, 9839-9864, 2011.

McDuffie, E. E., Smith, S. J., O'Rourke, P., Tibrewal, K., Venkataraman, C., Marais, E. A., Zheng, B., Crippa, M., Brauer, M., and Martin, R. V.: A global anthropogenic emission inventory of atmospheric pollutants from sector- and fuel-specific sources (1970–2017): an application of the Community Emissions Data System (CEDS), Earth Syst. Sci. Data, 12, 3413-3442, 2020.

Miyazaki, K., Eskes, H., Sudo, K., Boersma, K. F., Bowman, K., and Kanaya, Y.: Decadal changes in global surface NOx emissions from multi-constituent satellite data assimilation, Atmos. Chem. Phys., 17, 807-837, 2017.

Mo, Z., Shao, M., and Lu, S.: Compilation of a source profile database for hydrocarbon and OVOC emissions in China, Atmospheric Environment, 143, 209-217, 2016.

Paliwal, U., Sharma, M., and Burkhart, J. F.: Monthly and spatially resolved black carbon emission inventory of India: uncertainty analysis, Atmos. Chem. Phys., 16, 12457-12476, 2016.

Phillips, D.: Ambient Air Quality Synergies with a 2050 Carbon Neutrality Pathway in South Korea, Climate, 10, 1, 2022.

Qu, Z., Henze, D. K., Li, C., Theys, N., Wang, Y., Wang, J., Wang, W., Han, J., Shim, C., Dickerson, R. R., and Ren, X.: SO2 Emission Estimates Using OMI SO2 Retrievals for 2005–2017, Journal of Geophysical Research: Atmospheres, 124, 8336-8359, 2019.

1074 Saari, R. K., Selin, N. E., Rausch, S., and Thompson, T. M.: A self-consistent method to assess
1075 air quality co-benefits from U.S. climate policies, Journal of the Air & Waste Management
1076 Association, 65, 74-89, 2015.

1077 Samset, B. H., Lund, M. T., Bollasina, M., Myhre, G., and Wilcox, L.: Emerging Asian aerosol
1078 patterns, Nature Geoscience, 12, 582-584, 2019.

1079 Shan, Y., Huang, Q., Guan, D., and Hubacek, K.: China CO2 emission accounts 2016–2017,
1080 Scientific Data, 7, 54, 2020.

1081 Shi, Y. and Yamaguchi, Y.: A high-resolution and multi-year emissions inventory for biomass
1082 burning in Southeast Asia during 2001–2010, Atmospheric Environment, 98, 8-16, 2014.

1083 Shibata, Y. and Morikawa, T.: Review of the JCAP/JATOP Air Quality Model Study in Japan,
1084 Atmosphere, 12, 943, 2021.

1085 Simon, H., Beck, L., Bhave, P. V., Divita, F., Hsu, Y., Luecken, D., Mobley, J. D., Pouliot, G.
1086 A., Reff, A., Sarwar, G., and Strum, M.: The development and uses of EPA's SPECIATE
1087 database, Atmospheric Pollution Research, 1, 196-206, 2010.

1088 Song, Y., Liu, B., Miao, W., Chang, D., and Zhang, Y.: Spatiotemporal variation in
1089 nonagricultural open fire emissions in China from 2000 to 2007, Global Biogeochemical Cycles,
1090 23, 2009.

1091 Stavrakou, T., Müller, J.-F., Bauwens, M., and De Smedt, I.: Sources and Long-Term Trends of
1092 Ozone Precursors to Asian Pollution. In: Air Pollution in Eastern Asia: An Integrated
1093 Perspective, Bouarar, I., Wang, X., and Brasseur, G. P. (Eds.), Springer International Publishing,
1094 Cham, 2017.

1095 Sun, W., Shao, M., Granier, C., Liu, Y., Ye, C. S., and Zheng, J. Y.: Long-Term Trends of
1096 Anthropogenic SO2, NOx, CO, and NMVOCs Emissions in China, Earth's Future, 6, 1112-1133,
1097 2018.

1098 Takahashi, M., Feng, Z., Mikhailova, T. A., Kalugina, O. V., Shergina, O. V., Afanasieva, L. V.,
1099 Heng, R. K. J., Majid, N. M. A., and Sase, H.: Air pollution monitoring and tree and forest
1100 decline in East Asia: A review, Science of The Total Environment, 742, 140288, 2020.

1101 Van Damme, M., Clarisse, L., Franco, B., Sutton, M. A., Erisman, J. W., Wichink Kruit, R., van
1102 Zanten, M., Whitburn, S., Hadji-Lazaro, J., Hurtmans, D., Clerbaux, C., and Coheur, P.-F.:
1103 Global, regional and national trends of atmospheric ammonia derived from a decadal (2008–
1104 2018) satellite record, Environmental Research Letters, 16, 055017, 2021.

1105 van der A, R. J., Mijling, B., Ding, J., Koukouli, M. E., Liu, F., Li, Q., Mao, H., and Theys, N.:
1106 Cleaning up the air: effectiveness of air quality policy for SO2 and NOx emissions in China,
1107 Atmos. Chem. Phys., 17, 1775-1789, 2017.

1108 van der Werf, G. R., Randerson, J. T., Giglio, L., van Leeuwen, T. T., Chen, Y., Rogers, B. M.,
1109 Mu, M., van Marle, M. J. E., Morton, D. C., Collatz, G. J., Yokelson, R. J., and Kasibhatla, P. S.:
1110 Global fire emissions estimates during 1997–2016, Earth Syst. Sci. Data, 9, 697-720, 2017.

1111 von Schneidemesser, E. and Monks, P. S.: Air quality and climate – synergies and trade-offs,
1112 Environmental Science: Processes & Impacts, 15, 1315-1325, 2013.

1113 Wong, C.-M., Vichit-Vadakan, N., Kan, H., and Qian, Z.: Public Health and Air Pollution in
1114 Asia (PAPA): A Multicity Study of Short-Term Effects of Air Pollution on Mortality,
1115 Environmental Health Perspectives, 116, 1195-1202, 2008.

1116 Woo, J.-H., Choi, K.-C., Kim, H. K., Baek, B. H., Jang, M., Eum, J.-H., Song, C. H., Ma, Y.-I.,
1117 Sunwoo, Y., Chang, L.-S., and Yoo, S. H.: Development of an anthropogenic emissions
1118 processing system for Asia using SMOKE, Atmospheric Environment, 58, 5-13, 2012.

1119 Xiao, Q., Li, M., Liu, H., Fu, M., Deng, F., Lv, Z., Man, H., Jin, X., Liu, S., and He, K.:
1120 Characteristics of marine shipping emissions at berth: profiles for particulate matter and volatile
1121 organic compounds, Atmos. Chem. Phys., 18, 9527-9545, 2018.

1122 Xie, Y., Dai, H., Xu, X., Fujimori, S., Hasegawa, T., Yi, K., Masui, T., and Kurata, G.: Co-
1123 benefits of climate mitigation on air quality and human health in Asian countries, Environment
1124 International, 119, 309-318, 2018.

1125 Yin, L., Du, P., Zhang, M., Liu, M., Xu, T., and Song, Y.: Estimation of emissions from biomass
1126 burning in China (2003–2017) based on MODIS fire radiative energy data, Biogeosciences, 16,
1127 1629-1640, 2019.

1128 Yuan, B., Shao, M., Lu, S., and Wang, B.: Source profiles of volatile organic compounds
1129 associated with solvent use in Beijing, China, Atmospheric Environment, 44, 1919-1926, 2010.

1130 Zhang, C., Liu, C., Hu, Q., Cai, Z., Su, W., Xia, C., Zhu, Y., Wang, S., and Liu, J.: Satellite UV-
1131 Vis spectroscopy: implications for air quality trends and their driving forces in China during
1132 2005–2017, Light: Science & Applications, 8, 100, 2019.

1133 Zhang, Q., Streets, D. G., Carmichael, G. R., He, K. B., Huo, H., Kannari, A., Klimont, Z., Park,
1134 I. S., Reddy, S., Fu, J. S., Chen, D., Duan, L., Lei, Y., Wang, L. T., and Yao, Z. L.: Asian
1135 emissions in 2006 for the NASA INTEX-B mission, Atmos. Chem. Phys., 9, 5131-5153, 2009.

1136 Zhang, Y., Cooper, O. R., Gaudel, A., Thompson, A. M., Nédélec, P., Ogino, S.-Y., and West, J.
1137 J.: Tropospheric ozone change from 1980 to 2010 dominated by equatorward redistribution
1138 of emissions, Nature Geoscience, 9, 875-879, 2016.

1139 Zhang, Y., West, J. J., Emmons, L. K., Flemming, J., Jonson, J. E., Lund, M. T., Sekiya, T.,
1140 Sudo, K., Gaudel, A., Chang, K.-L., Nédélec, P., and Thouret, V.: Contributions of World
1141 Regions to the Global Tropospheric Ozone Burden Change From 1980 to 2010, Geophysical
1142 Research Letters, 48, e2020GL089184, 2021.

1143 Zhao, Y., Nielsen, C. P., Lei, Y., McElroy, M. B., and Hao, J.: Quantifying the uncertainties of a
1144 bottom-up emission inventory of anthropogenic atmospheric pollutants in China, Atmos. Chem.
1145 Phys., 11, 2295-2308, 2011.

1146 Zhao, Y., Nielsen, C. P., McElroy, M. B., Zhang, L., and Zhang, J.: CO emissions in China:
1147 Uncertainties and implications of improved energy efficiency and emission control, Atmospheric
1148 Environment, 49, 103-113, 2012.

1149 Zhao, Y., Zhang, J., and Nielsen, C. P.: The effects of recent control policies on trends in
1150 emissions of anthropogenic atmospheric pollutants and CO_2 in China, Atmos.
1151 Chem. Phys., 13, 487-508, 2013.

1152 Zheng, B., Cheng, J., Geng, G., Wang, X., Li, M., Shi, Q., Qi, J., Lei, Y., Zhang, Q., and He, K.:
1153 Mapping anthropogenic emissions in China at 1 km spatial resolution and its application in air
1154 quality modeling, Science Bulletin, 66, 612-620, 2021.

1155 Zheng, B., Chevallier, F., Yin, Y., Ciais, P., Fortems-Cheiney, A., Deeter, M. N., Parker, R. J.,
1156 Wang, Y., Worden, H. M., and Zhao, Y.: Global atmospheric carbon monoxide budget 2000–
1157 2017 inferred from multi-species atmospheric inversions, Earth Syst. Sci. Data, 11, 1411-1436,
1158 2019.

1159 Zheng, B., Huo, H., Zhang, Q., Yao, Z. L., Wang, X. T., Yang, X. F., Liu, H., and He, K. B.:
1160 High-resolution mapping of vehicle emissions in China in 2008, Atmos. Chem. Phys., 14, 9787-
1161 9805, 2014.

1162 Zheng, B., Tong, D., Li, M., Liu, F., Hong, C., Geng, G., Li, H., Li, X., Peng, L., Qi, J., Yan, L.,
1163 Zhang, Y., Zhao, H., Zheng, Y., He, K., and Zhang, Q.: Trends in China's anthropogenic
1164 emissions since 2010 as the consequence of clean air actions, Atmos. Chem. Phys., 18, 14095-
1165 14111, 2018.

1166 Zhou, Y., Xing, X., Lang, J., Chen, D., Cheng, S., Wei, L., Wei, X., and Liu, C.: A
1167 comprehensive biomass burning emission inventory with high spatial and temporal resolution in
1168 China, Atmos. Chem. Phys., 17, 2839-2864, 2017.

1169